表　感染症の鑑別

	細菌	ウイルス	クラミジア	アレルギー
自覚症状	眼脂（3＋） 流涙（2＋）	眼脂（＋） 流涙（3＋）	眼脂（3＋） 流涙（3＋）	かゆみ（3＋） 流涙（2＋）
潜伏期	1～3日	5～14日	5～12日	
結膜所見	カタル性	濾胞性	濾胞性	乳頭増殖
耳前リンパ節腫脹	＋－	＋＋	＋＋	－
感染力	＋－	＋＋	＋＋	－

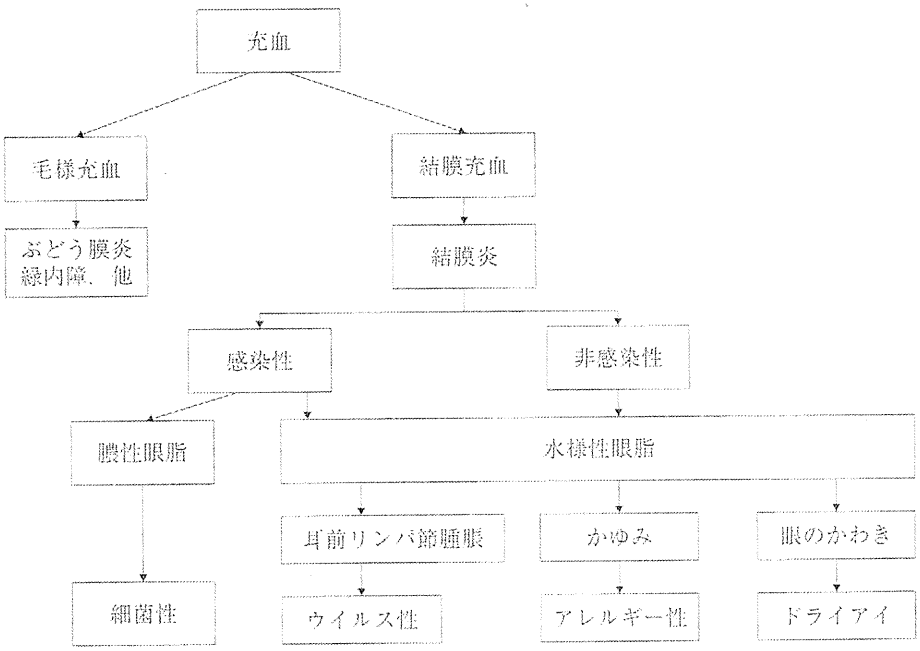

図　結膜炎の診断

が増加する。アレルギー性結膜炎にはアトピー性結膜炎，春季カタル，巨大乳頭結膜炎，花粉症などが含まれるが，急性結膜炎として発症するのは主に花粉症である。日本での罹患者は2,000万人もあり，季節性のあるのが特徴である。近年アレルギー性結膜炎発症時期の低年齢化がすすんでいる。アレルギーの原因で最も多いのは，スギ花粉であるが，その他カモガヤ，ブタクサ，ヒノキなども原因となる。花粉の飛ぶ時期がそれぞれ異なるため，春だけでなく，秋にも花粉症が見られる。通年性のアレルギー源として，ハウスダストやダニがあげられる。アレルギー性結膜炎の症状はかゆみが主であるが，かゆみのために眼をこすると，激しい結膜浮腫を来すことがある（表，図）。

II．重症度

結膜炎の原因と重症度は年齢によって異なる。成人では軽症の結膜炎でも，新生児では重症の結膜炎となり，全身症状を伴うこともある。また，ウイルス性結膜炎では角膜炎を引き起こすことがあり，恒久的な視力障害を残すことがある。ウイルス性結膜炎では，眼瞼結膜の濾胞形成が見られるが，新生児では濾胞形成でなく偽膜を作ってしまうことがあ

る。偽膜によって眼球結膜と眼瞼結膜が癒着すると眼球運動障害を呈することがある。

III. 原因別による私の処方（第1・第2選択薬，用法・用量）

細菌性結膜炎では，起炎菌に有効な抗生物質の投与を行う。クラミジア結膜炎には，ニューキノロン系抗菌薬（オゼックス®など）の頻回点眼，あるいはタリビッド®眼軟膏1日5回点入を行う。もっとも頻度の高いインフルエンザ菌，肺炎球菌をターゲットにする場合には，広範囲の抗菌スペクトルを有するニューキノロン系抗菌薬（オゼックス®，クラビット®）1回1滴，1日3回点眼を行う。

アデノウイルス性結膜炎に対しては，特別な抗ウイルス薬はなく，混合感染予防のために抗菌点眼薬を用いる。症状が劇症で角膜炎を伴うときにはステロイド点眼薬（リンデロン®点眼液）を用いる。もっとも重要なことは伝染予防対策であり，流水での手洗い，ペーパータオルの使用，学校への出席停止の厳守などである。

アレルギー性結膜炎では，非ステロイド系の抗アレルギー剤（パタノール®1日4回）を投与する。重篤なアレルギー性結膜炎では副腎皮質ステロイド（0.1%フルメトロン®点眼液1日4回）や免疫抑制剤（パピロックミニ®点眼液1日4回）の投与を行う。非眼科医による安易な副腎皮質ステロイドの投与は避けるべきである。

IV. 処方のポイント（治療）

抗菌薬投与による耐性菌の出現に注意が必要である。

V. 副作用とその対策

抗菌薬の重篤な副作用は少なく，眼刺激感，眼周囲についたときのかぶれなどである。

VI. 注意が必要な点

もっとも注意が必要な点としては，結膜炎以外にも充血を主訴とする眼疾患が多数存在することである。角膜炎，虹彩炎，緑内障などでは毛様充血を来す。眼脂を伴わない点，眼瞼結膜に充血がみられない点で結膜炎と異なり，これらを見た場合には眼科医に紹介すべきである。安易に副腎皮質ステロイドの処方を行うと，一時的に症状の改善がみられることが多く，確定診断に難渋することがある。

VII. 治らない患児への対応

ウイルス性結膜炎でなければ，治療によって3日以内に症状の改善があるはずである。眼脂が多い他の疾患として，涙嚢炎や麦粒腫などがあるため，3日以内に改善が見られない場合には眼科医に紹介すべきである。

☆　☆　☆　☆　☆　☆

Negative regulation of ciliary length by ciliary male germ cell-associated kinase (Mak) is required for retinal photoreceptor survival

Yoshihiro Omori[a,b], Taro Chaya[a,b], Kimiko Katoh[a], Naoko Kajimura[c], Shigeru Sato[a,d], Koichiro Muraoka[a], Shinji Ueno[e], Toshiyuki Koyasu[e], Mineo Kondo[e], and Takahisa Furukawa[a,b,1]

[a]Department of Developmental Biology and [b]Japan Science and Technology Agency, Core Research for Evolutional Science and Technology, Osaka Bioscience Institute, 6-2-4 Furuedai, Suita, Osaka 565-0874, Japan; [c]Research Center for Ultra-High Voltage Electron Microscopy, Osaka University, 7-1 Mihogaoka, Ibaraki, Osaka 567-0047, Japan; [d]Department of Ophthalmology, Osaka University Graduate School of Medicine, 2-2 Yamadaoka, Suita, Osaka 565-0871, Japan; and [e]Department of Ophthalmology, Nagoya University Graduate School of Medicine, 65 Tsuruma-cho, Showa-ku, Nagoya 466-8550, Japan

Edited by Jeremy Nathans, The Johns Hopkins University, Baltimore, MD, and approved November 12, 2010 (received for review June 30, 2010)

Cilia function as cell sensors in many organs, and their disorders are referred to as "ciliopathies." Although ciliary components and transport machinery have been well studied, regulatory mechanisms of ciliary formation and maintenance are poorly understood. Here we show that male germ cell-associated kinase (Mak) regulates retinal photoreceptor ciliary length and subcompartmentalization. Mak was localized both in the connecting cilia and outer-segment axonemes of photoreceptor cells. In the *Mak*-null retina, photoreceptors exhibit elongated cilia and progressive degeneration. We observed accumulation of intraflagellar transport 88 (IFT88) and IFT57, expansion of kinesin family member 3A (Kif3a), and acetylated α-tubulin signals in the *Mak*-null photoreceptor cilia. We found abnormal rhodopsin accumulation in the *Mak*-null photoreceptor cell bodies at postnatal day 14. In addition, overexpression of retinitis pigmentosa 1 (RP1), a microtubule-associated protein localized in outer-segment axonemes, induced ciliary elongation, and Mak coexpression rescued excessive ciliary elongation by RP1. The RP1 N-terminal portion induces ciliary elongation and increased intensity of acetylated α-tubulin labeling in the cells and is phosphorylated by Mak. These results suggest that Mak is essential for the regulation of ciliary length and is required for the long-term survival of photoreceptors.

Cilia are evolutionally conserved microtubule-based organelles that extend from basal bodies and form on the apical surface of cells. In humans, ciliary dysfunction is associated with various diseases that can be broadly classified as "ciliopathies." As exemplified by Bardet-Biedl syndrome (BBS), diseases linked with a defect in the primary cilia usually are associated with a broad spectrum of pathologies, including polydactyly, craniofacial abnormalities, brain malformation, situs inversus, obesity, diabetes, polycystic kidney, and retinal degeneration (1, 2). In vertebrates, many types of cells in the G1 phase develop cilia, but ciliary length varies in each cell type of different tissues (3). Retinal photoreceptor cells develop a light-sensory structure containing photopigments and light-transducing machinery, the outer segment. Outer segments are formed initially from the primary cilia in photoreceptor precursors (4, 5). The photoreceptor cilium is divided structurally into at least two subcompartments: the connecting cilia, distal to the basal body, and the axoneme in the outer segment, distal to the connecting cilia. The connecting cilium is analogous to the transitional zone of the motile cilia (6, 7). Connecting cilium connects the inner and outer segments of photoreceptors and is essential for protein transport between the inner and outer segments. Defects of the photoreceptor ciliary transport machinery (called "intraflagellar transport," IFT) cause photoreceptor degeneration in model animals (8–10). The retinitis pigmentosa 1 (RP1) protein is localized specifically in the outer-segment axonemes in photoreceptors, which stabilizes cytosolic microtubules (11). A mutation in human *RP1* generating a deletion of the RP1 C-terminal portion causes dominant retinitis pigmentosa (12).

Mechanisms of ciliogenesis have been well studied in the green algae *Chlamydomonas reinhardtii*. The *Chlamydomonas LF4* mutant shows a long-flagella phenotype. *LF4* encodes a protein highly similar to mammalian male germ cell-associated kinase (Mak) and intestinal cell kinase (ICK) (13). Loss of function of the *LF4* homologs *Caenorhabditis elegans dye-filling defective 5* (*Dyf-5*) and *Leishmania Mexicana LmxMPK9* also causes slightly elongated cilia or flagella (14, 15). However, molecular regulatory mechanisms controlling ciliary length remain unknown. *Mak* was first identified as a gene highly expressed in testicular germ cells (16). Spermatogenesis of the *Mak*-KO mouse is intact (17). In addition to expression in the testis, *Mak* is also expressed in the retina (18, 19). However, the molecular function of Mak in the retina has not been reported yet.

Results

***Mak* Is Expressed in Photoreceptors in the Retina.** In the course of a microarray screening for genes specifically expressed in photoreceptors (20), we found that the *Mak* transcript is markedly reduced in the orthodenticle homeobox 2 (Otx2) conditional knockout (CKO) retina in which most of the photoreceptors are converted to amacrine-like cells (21). We confirmed by quantitative PCR analysis that *Mak* expression is markedly decreased in the *Otx2* CKO retina at postnatal day 12 (P12) (Fig. S1*A*). From a retinal cDNA library we cloned an alternatively spliced form of *Mak* full-length cDNA containing a 75-bp in-frame insertion to the reported *Mak* cDNA (19) (Fig. S2). RT-PCR analysis revealed that this form is likely to be the major alternatively spliced form of the *Mak* transcript in the retina (four of six clones analyzed). To investigate *Mak* expression in the developing retina, we performed in situ hybridization analysis using a *Mak* probe (Fig. 1 *A* and *B* and Fig. S1 *B–D*). *Mak* expression was detected first at embryonic day 15.5 (E15.5) in the outer part of the neuroblastic layer (NBL), corresponding to photoreceptor precursors (Fig. 1*A*). *Mak* expression was restricted to the photoreceptor layer after birth (Fig. 1*B* and Fig. S1 *C* and *D*). These results indicate that *Mak* is expressed predominantly in photoreceptor cells in the retina.

Mak Is Localized in the Photoreceptor Connecting Cilia and Outer-Segment Axonemes. To investigate the subcellular localization of Mak in photoreceptor cells, we immunostained retinal sections using an anti-Mak antibody. To eliminate cross-reaction with other kinases, we raised an antibody which recognizes the C-terminal portion of Mak. We confirmed that the anti-Mak antibody

Author contributions: Y.O. and T.F. designed research; Y.O., T.C., K.K., N.K., S.S., K.M., S.U., T.K., M.K., and T.F. performed research; Y.O. and T.F. contributed new reagents/analytic tools; Y.O., T.C., K.K., N.K., S.S., K.M., S.U., T.K., and M.K. analyzed data; and Y.O. and T.F. wrote the paper.

The authors declare no conflict of interest.

This article is a PNAS Direct Submission.

Freely available online through the PNAS open access option.

[1]To whom correspondence should be addressed. E-mail: furukawa@obi.or.jp.

This article contains supporting information online at www.pnas.org/lookup/suppl/doi:10.1073/pnas.1009437108/-/DCSupplemental.

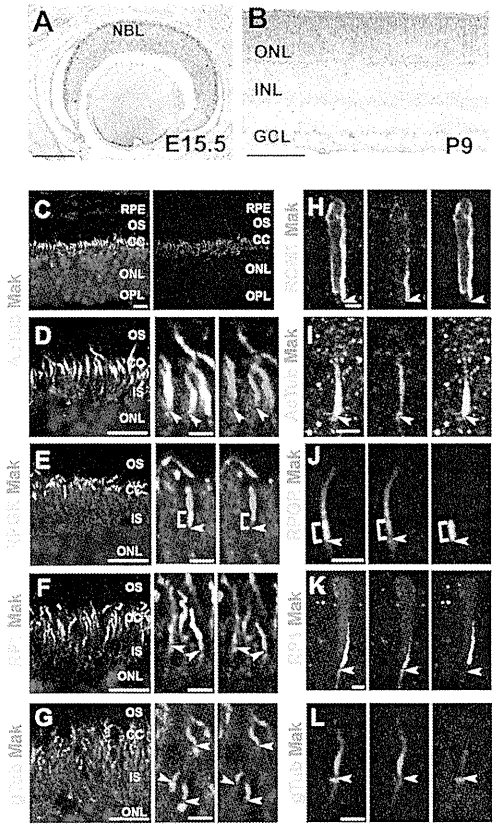

Fig. 1. Expression and subcellular localization of Mak in the retina. (*A* and *B*) In situ hybridization analysis of retinal sections at E15.5 (*A*) and postnatal day 9 (P9) (*B*). *Mak* mRNA is expressed in both photoreceptor precursors and developing photoreceptors in the retina. (*C–L*) Subcellular localization of Mak in photoreceptors. Retinal sections at P14 (*E*) and 1 mo (*C*, *D*, *F*, and *G*) and dissociated photoreceptor cells at P14 (*H–L*) were stained with anti-Mak (red in *C–L*) and anti-acetylated α-tubulin (a marker for cilia; green in *C*, *D*, and *I*), anti-RPGR (a marker for connecting cilia; green in *E* and *J*), anti-RP1 (a marker for outer-segment axonemes; green in *F* and *K*), anti-ROM1 (a marker for outer-segment disks, green in *H*), or anti-γ-tubulin (a marker for basal bodies; green in *G* and *L*) antibodies. [Scale bars: 100 μm (*A* and *B*), 2 μm (*H–L* and *D–G Center* and *Right*), and 10 μm (*C* and *D–G Left*).] Arrowheads (*D–L*) indicate basal body-connecting cilium junctions. Brackets (*E* and *J*) indicate connecting cilia. CC, connecting cilia; GCL, ganglion cell layer; INL, inner nuclear layer; IS, inner segments; NBL, neuroblastic layer; ONL, outer nuclear layer; OPL, outer plexiform layer OS, outer segments; RPE, retinal pigment epithelium.

recognizes the major retinal variant of Mak with the 25-amino acid insertion (Fig. S1*E*). By immunostaining, we observed a layer of Mak signals between the retinal pigment epithelia and outer nuclear layer (ONL) corresponding to the photoreceptor cilia (Fig. 1*C*).

To identify the precise localization of Mak in the photoreceptor cilia, we immunostained the retina using the Mak antibody along with other ciliary markers including acetylated α-tubulin (a ciliary marker), retinitis pigmentosa GTPase regulator (RPGR, a connecting cilium marker) (7), RP1 (a marker for the outer-segment axonemes) (11), and rod outer-segment membrane protein 1 (ROM1, a marker for the outer-segment disks) (Fig. 1 *C–L*) (22). The Mak signal was observed broadly in the photoreceptor cilia overlapping with ROM1, RPGR, RP1 and acetylated α-tubulin signals (Fig. 1 *C–F* and *H–K*; for summary, see Fig. S9). We observed a slight signal of Mak overlapping with the γ-tubulin signal, a marker for basal bodies (Fig. 1 *G* and *L*). These results indicate that Mak is localized in both the connecting cilia and the outer-segment axonemes. Interestingly, the intensity of the Mak signal was not uniform in the photoreceptor cilia. The decreased Mak signal was observed in the proximal portion of the connecting cilia (Fig. 1 *E* and *J*) and the distal portion of the outer-segment axonemes (Fig. 1 *F* and *K*).

Photoreceptors Degenerate Progressively in the *Mak*-Deficient Retina. *Mak*-null mice were established previously, and it was reported that *Mak* is not essential for spermatogenesis, although *Mak* is highly expressed in the testis (17). To investigate in vivo Mak function in the retina, we analyzed this KO mouse. We confirmed that none of the normal *Mak* transcripts, including the major retinal variant of *Mak* with a 75-bp insertion, were expressed in the *Mak*-KO retina (Fig. S1*F*). Until retinogenesis was complete in the normal retina at postnatal day 14 (P14), the *Mak*-KO retina exhibited normal layering and cell composition, indicating that loss of *Mak* does not affect cell fates (Fig. 2 *A* and *B* and Fig. S3 *A–F*). We also analyzed the retinas at age 1 mo, 6 mo, and 12 mo. Notably, we found progressive degeneration of the ONL (a photoreceptor layer) in the *Mak*-KO retina after 1 mo (Fig. 2 *C–I*). This progressive ONL loss often is observed in animal models of retinitis pigmentosa and Leber's congenital amaurosis (23–27). We observed no obvious structural differences between the heterozygous and wild-type retinas at 6 mo (Fig. S4 *A–C*). The thickness of the other layers did not differ in the *Mak*-KO and wild-type retinas (Fig. S5*A*).

To examine if loss of *Mak* in the retina affects photoreceptor function, we recorded electroretinograms (ERG) from adult *Mak*-KO mice at age 3 mo. Both scotopic and photopic ERG amplitudes of *Mak*-KO mice were significantly smaller than those of the control mice (Fig. 2*I* and Fig. S5 *B–D*). These results show that the loss of *Mak* impairs the function of both rods and cones.

Cilia Are Elongated in *Mak*-KO Photoreceptors. How does progressive photoreceptor death occur in the *Mak*-KO retina? To explore this question, we examined photoreceptors in the *Mak*-deficient retina by immunostaining using antibodies against photoreceptor ciliary markers. We first confirmed the loss of *Mak* in the photoreceptor cilia of the *Mak*-KO retina at P14 (Fig. 3 *A*, *A′*, *B*, and *B′*). Notably, we found that the cilia stained with the anti-acetylated α-tubulin antibody were markedly elongated in *Mak*-deficient rod photoreceptors (Fig. 3*B*). We measured ciliary length of rod photoreceptors and found that the acetylated α-tubulin–positive cilia in *Mak*-KO photoreceptors were approximately twice the length of wild-type cilia (Fig. 3 *K* and *L*). We also found that cone photoreceptor cilia were elongated in the *Mak*-null retina (Fig. S6 *A–D*). To investigate whether ciliary subcompartments are affected in *Mak*-KO photoreceptors, we immunostained for RPGR (a marker of the connecting cilia) in the *Mak*-KO retina. We observed an approximately twofold elongation of the RPGR-positive connecting cilia in the *Mak*-KO retina (Fig. 3 *C*, *D*, and *L* and Fig. S6*E*). In contrast, γ-tubulin staining (a basal body marker) showed no significant difference between *Mak*-KO and wild-type photoreceptors (Fig. 3 *C* and *D*). Next, we stained for RP1, a marker of the outer-segment axonemes. Unexpectedly, we observed excessively long acetylated α-tubulin labeling in the outer-segment axonemes (Fig. 3 *E* and *F*). In most of the wild-type photoreceptors, an acetylated α-tubulin signal is observed in less than half of the proximal portion of the RP1-positive outer-segment axoneme, whereas in the *Mak*-KO photoreceptors often almost all the outer-segment axoneme is acetylated α-tubulin signal-positive. The percentage of excessively long acetylated α-tubulin labeling of the outer-segment axonemes (wherein more than half of the distal portion of the outer-segment axoneme is acetylated α-tubulin signal-positive) is 5.1% (n = 59) in the wild-type photoreceptors, whereas in *Mak*-KO photoreceptors 83.3% (n = 66) of the axonemes have excessively long acetylated α-tubulin labeling. The distance from the top of the outer segment to the top of the outer-segment axonemes stained with acetylated α-tubulin decreased in *Mak*-KO photoreceptors (Fig. S6 *F* and *G*). These results demonstrate that loss of *Mak* affects both subcompartments of the cilia, the connecting cilia and outer-segment axonemes.

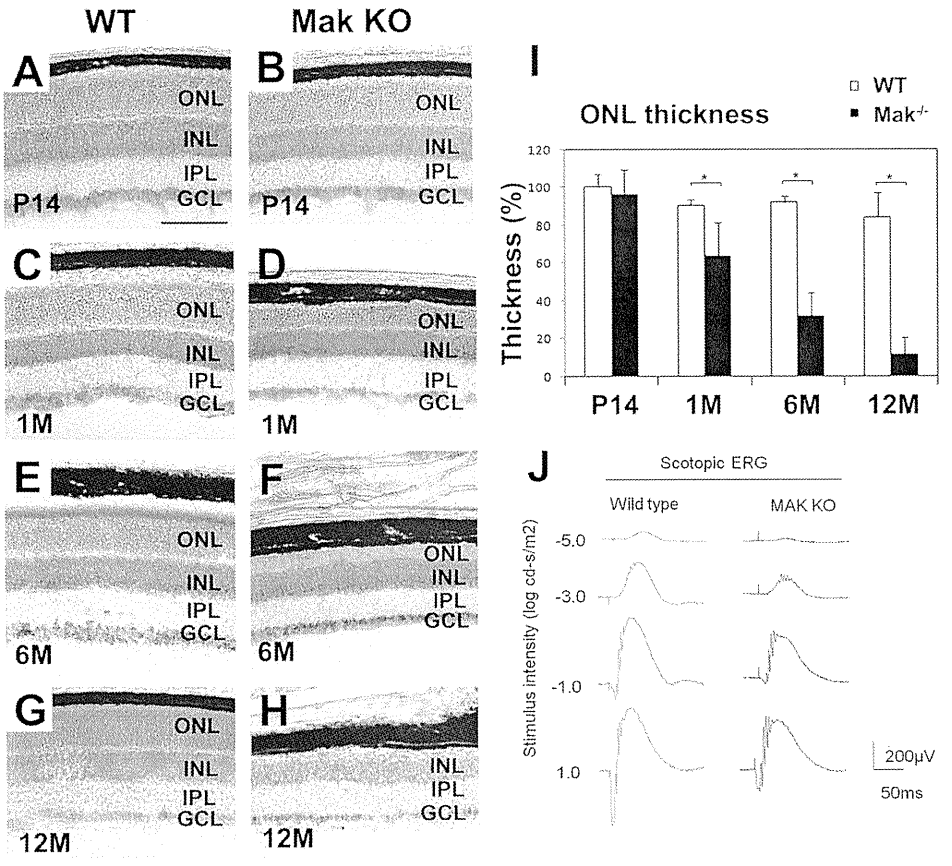

Fig. 2. Loss of *Mak* leads to photoreceptor degeneration (*A–H*). Retinal sections from wild-type and *Mak*-KO mice at age P14 (*A* and *B*), 1 mo (*C* and *D*), 6 mo (*E* and *F*), and 12 mo (*G* and *H*) were stained with toluidine blue. Progressive degeneration of the ONL (a photoreceptor layer) occurs in the *Mak*-KO retina. (Scale bar: 100 μm.) IPL, inner plexiform layer. (*I*) Thickness of retinal layers was measured at age P14, 1 mo, 6 mo, and 12 mo. ONL thickness decreased progressively in the *Mak*-KO retina. Average of layer thickness in the wild-type retina at P14 was set to 100%. Error bars show SD. $*P < 0.03$. (*J*) ERGs recorded from *Mak*-KO mice. Scotopic ERGs elicited by four different stimulus intensities (–5.0 to 1.0 log cd-s/m^2).

To examine whether loss of *Mak* affects the anterograde IFT and kinesin motors, we stained photoreceptor cilia with anti-IFT88, anti-IFT57, and anti-Kif3a antibodies. We observed that both IFT88 and IFT57 were concentrated on two portions, the tip of the connecting cilia at the outer-segment base and the basal part of the connecting cilia, as previously reported (28). Notably, in *Mak*-KO photoreceptors, we found that IFT88 and IFT57 were accumulated in outer-segment axonemes (Fig. 3 *G* and *H* and Fig. S6 *H* and *I*). In wild-type photoreceptors, the Kif3a staining overlaps with the acetylated α-tubulin staining and is concentrated on the basal part of the cilia (Fig. S6 *J* and *K*). In *Mak*-KO photoreceptors, the Kif3a staining extends along the elongated acetylated α-tubulin–positive cilia (Fig. S6 *J* and *K*). Interestingly, we also observed an accumulation of rhodopsin in the *Mak*-KO photoreceptor cell bodies at P14 (Fig. 3 *I*, *I′*, *J*, and *J′*).

Mak is expressed in epithelia of the nasal cavity and the testis (16, 19). Respiratory epithelia of the nasal cavity have multiple motile cilia which display the 9+2 microtubule structure. We observed Mak localizing in the cilia of the respiratory epithelia (Fig. S6*L*). The Mak signal is reduced in the *Mak*-KO nasal cavity (Fig. S6*M*). However, the ciliary length of respiratory epithelia did not differ in wild-type and *Mak*-KO mice (Fig. S6 *L–N*). Similarly, we also found that the acetylated-α-tubulin–positive flagellar length of epididymal sperm does not differ in wild-type and *Mak*-KO mice (Fig. S6 *O–Q*).

Aberrant Outer-Segment Disk Formation in *Mak*-Deficient Photoreceptors. The 9+0 axonemes of the photoreceptor cilia are assembled by nine peripheral doublet microtubules without a central microtubule (3). To test if loss of *Mak* affects ultrastructural microtubule organization in the photoreceptor cilia, we performed an electron microscopic analysis. We observed no significant change in ciliary ultrastructures, including the array of the 9+0 microtubule doublets in transverse sections of the connecting cilium in *Mak*-KO photoreceptors (Fig. S7 *A* and *B*). Consistent with the results of the immunofluorescent analysis, we found elongated connecting cilium in the *Mak*-KO photoreceptors at age 1 mo in a longitudinal section of the connecting cilia ($100 \pm 2\%$ in wild type, $n = 12$; $233 \pm 22\%$ in *Mak*-KO, $n = 9$; $P < 0.03$) (Fig. 3 *M* and *N*).

In both vertebrate photoreceptors and nematode amphid channel cilia, the proximal microtubules of the axonemes are doublets, whereas distal microtubules are singlets (29, 30). In the distal segment of the amphid channel cilia in *dyf-5* animals, singlet microtubules were observed (14). We observed singlet microtubules in outer-segment axonemes, which are positioned near the disk clefts, in both wild-type and Mak-null retinas (Fig. S7 *C–F*).

We observed severely disorganized *Mak*-KO outer segments at age 1 mo compared with the wild type (Fig. 3 *M* and *N*). In contrast, disk rim formation seems to be intact in the *Mak*-null outer segments at age 1 mo (Fig. S7 *G* and *H*). To examine whether the outer-segment disorganization observed in Mak-deficient retinas is caused by a developmental defect or degeneration after normal development, we observed photoreceptor outer segments at P14 by electron microscopy. At this stage, the outer segments are still developing (31). In wild-type photoreceptors, the stack of disk membranes in the outer segments is oriented perpendicular to the long axis of the outer segments (Fig. S7 *I* and *I′*). In the *Mak*-KO retina, however, we observed that the disk membranes were frequently oriented obliquely or parallel to the long axis of the outer segments (Fig. S7 *J* and *J′*). In addition, the disk diameters are approximately two to four times larger in *Mak*-null than in wild-type outer segments (Fig. S7 *I′* and *J′*). Enlarged disks oriented obliquely or parallel to the long axis of photoreceptors were reported in mutant mice including *RP1*-mutant and *RPGRIP1*-null mice (24, 25). These results suggest the disorganization of the outer segment observed in the *Mak*-KO retinas is, at least partially, the result of a developmental defect in outer-segment formation.

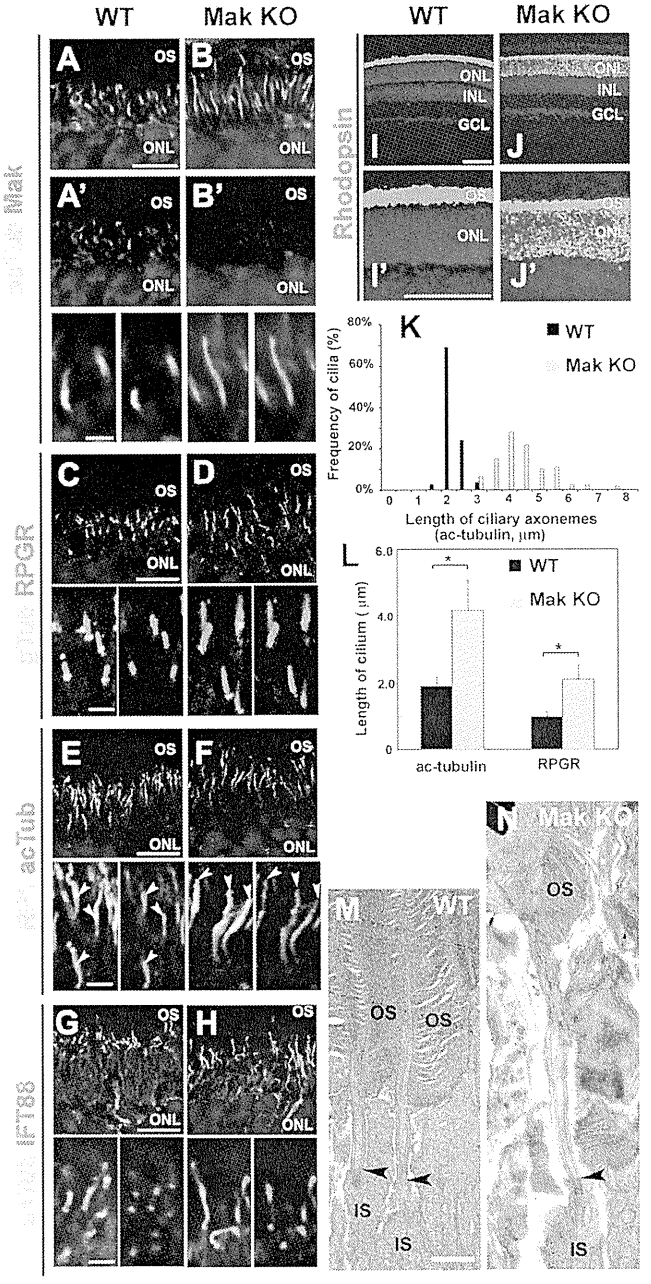

Fig. 3. Ciliary defect in *Mak*-null photoreceptors. (*A–H*) Immunohistochemical analysis of the *Mak*-null photoreceptor cilia. Retinal sections from wild-type mice (*A*, *A′*, *C*, *E*, and *G*) and *Mak*-KO mice (*B*, *B′*, *D*, *F*, and *H*) at age P14 (*A*, *A′*, *B*, and *B′*) and 1 mo (*C–H*) were stained with anti-Mak (red in *A*, *A′*, *B*, and *B′*), anti-acetylated α-tubulin (a ciliary marker; green in *A*, *B*, *G*, and *H*; red in *E* and *F*), anti-RPGR (a connecting cilium marker; red in *C* and *D*), anti-RP1 (a marker for the outer-segment axonemes; green in *E* and *F*), anti-IFT88 (a component of IFT complex; red in *G* and *H*) or anti–γ-tubulin (a marker for the basal bodies; green in *C* and *D*) antibodies. Arrowheads in *E* and *F* indicate the distal tips of acetylated microtubules in the outer-segment axonemes. (*I* and *J*) Rhodopsin is mislocalized in the *Mak*-KO retina. Retinal sections from wild-type mice (*I* and *I′*) and *Mak*-KO mice (*J* and *J′*) at age P14 were stained with an anti-rhodopsin antibody. [Scale bars: 10 μm (*A*, *C*, *E*, and *G*, *Upper*), 100 μm (*I* and *I′*), and 2 μm (*A′*, *C*, *E*, and *G*, *Lower*).] (*K* and *L*) Length of the ciliary axonemes stained with the anti-acetylated α-tubulin antibody (*K* and *L*) and connecting cilia stained with the anti-RPGR (*L*) antibody in the wild-type photoreceptors (black bars) and *Mak*-KO photoreceptors (gray bars) were measured. Error bars show SE. $*P < 0.03$. (*M* and *N*) Longitudinal profiles of the connecting cilia in 1-mo-old wild-type photoreceptors (*M*) and *Mak*-KO photoreceptors (*N*) observed by electron microscopy. Arrowheads indicate the basal body-connecting cilium junctions in the photoreceptors. (Scale bar in *M*: 1 μm.)

Mak Overexpression Reduces Ciliary Elongation in Cultured Cells. To investigate the mechanisms by which Mak regulates ciliary length, we established a cultured cell system in which NIH 3T3 fibroblast cells develop cilia at a high frequency within 24 h after serum starvation (Fig. S8). We prepared FLAG-tagged constructs expressing a full-length wild-type Mak (*Mak-WT*), a kinase-dead mutant Mak (*Mak-KD*), and a deletion-mutant Mak lacking the C-terminal nonkinase domain (*Mak-N*) (Fig. S8*F*). The *Mak-KD* construct was generated by replacing a lysine residue (K33) located in the ATP-binding pocket of the Mak kinase domain with an arginine residue (32).

We transfected these constructs into NIH 3T3 cells and measured ciliary length. We found that the cells transfected with the wild-type *Mak* construct had shorter cilia than cells transfected with the control constructs (Fig. S8 *A*, *B*, and *G*). On the other hand, cells transfected with the *Mak-KD* or *Mak-N* construct showed no significant change in ciliary length (Fig. S8 *D*, *E*, and *G*), showing that kinase activity and/or the C-terminal region of Mak is essential for the regulation of ciliary length.

We then investigated the subcellular localization of Mak in transfected cells using an anti-FLAG antibody. We observed that *Mak-WT* was localized mainly in the nuclei as previously reported (32). As expected from the ciliary localization of Mak in photoreceptors, we observed that *Mak-WT* is also localized in the cilia of transfected cells. Mak localization was restricted to the tip of the shortened cilia (Fig. S8*B*). Although we rarely observed elongated cilia in *Mak-WT*–transfected cells, ciliary tip localization of *Mak-WT* was observed in those cells (Fig. S8*C*). We found that *Mak-KD* is also localized at the ciliary tip, suggesting that kinase activity is not required for the ciliary localization of Mak. In contrast, *Mak-N* was not localized in the cilia, showing that the C-terminal portion of Mak is essential for the ciliary localization of Mak.

RP1 Induces Ciliary Elongation and Reduces the Effect of Mak Overexpression. It was previously reported that knock-in mice with a partial deletion of the *RP1* gene exhibited shorten cilia (24). As we described above, we found colocalization of Mak with RP1 in the ciliary axoneme of wild-type photoreceptors. *Mak*-KO photoreceptors exhibited excessively long acetylated α-tubulin labeling. These observations prompted us to investigate whether RP1 is involved in the mechanisms by which Mak regulates ciliary length. To do so, we prepared constructs expressing RP1 and transfected them with or without the Mak-expressing constructs (Fig. 4*A*). We observed increased ciliary length in the cells transfected with full-length RP1 (*RP1-FL*) (Fig. 4 *B–E*, *J*, and *K*). In humans, the mutations in the *RP1* gene generating deletion of the C-terminal portion of RP1 cause dominant retinitis pigmentosa (12). Interestingly, the intensity of acetylated α-tubulin labeling significantly increased in cells expressing the N-terminal RP1 (RP1-N) construct containing the doublecortin domain, indicating that the cytoplasmic microtubules are more stable in these cells (Fig. 4 *F–I*). Coimmunostaining of FLAG-tag with acetylated α-tubulin showed that RP1-FL and RP1-N were localized in a large portion of the distal cilia but not in the basal cilia, a putative transition zone (Fig. 4 *E* and *G*). These results suggest that RP1 is a positive regulator of ciliary length. Notably, cotransfection of *Mak* with *RP1-FL* or *RP1-N* constructs rescued the excessive elongation of the cilia (Fig. 4 *J* and *K*). This result suggests that a functional balance between Mak and RP1 is essential for the regulation of ciliary length and proper formation of the ciliary subcompartments. To test whether Mak rescues increased acetylated α-tubulin signals in cells expressing RP1-N, we cotransfected Mak with an RP1-N construct and observed the acetylated α-tubulin signal levels in the cells. We found that expression of Mak significantly decreased the intensity of acetylated α-tubulin labeling in the cells expressing RP1-N (Fig. S8 *H–J*).

To assess whether Mak physically interacts with RP1, we performed an immunoprecipitation assay. We expressed Mak and FLAG-tagged full-length RP1 or RP1-N in HEK293 cells and performed an immunoprecipitation with an anti-FLAG antibody. We found specific interactions of Mak with both RP1-FL and RP1-N (Fig. 4*L*).

Then, to examine the possibility that Mak directly phosphorylates RP1, we performed a kinase assay using purified GST-Mak. Interestingly, we found that GST-RP1-N was markedly phosphorylated by Mak, whereas no obvious phosphorylation of the GST-RP1 C-terminal (GST-RP1-C1) construct or GST alone was detected (Fig. 4*M*). We observed weak phosphorylation of GST-RP1-C2 by Mak. To characterize the kinase activity of Mak with the RP1-N substrate, we performed a kinetic analysis. We found that the K_m value for ATP was 19 μM (Fig. S8*K*). In addition, we confirmed that Mak-phosphorylated RP1-N was dephosphorylated by λ-phosphatase (Fig. S8*L*). These results support the idea that RP1 is a phosphorylation target of Mak.

Discussion

In the current study, we show that Mak is essential for preventing excessive elongation of the cilia and for maintenance of photoreceptor cells. Our observations in the *Mak*-KO retina suggest that a negative regulatory mechanism of ciliary length is essential for long-term photoreceptor survival, suggesting that this mechanism is involved in the pathogenesis of human photoreceptor degenerative diseases such as retinitis pigmentosa, Leber's congenital amaurosis, and BBS. In addition, similar negative regulatory mechanisms of ciliary length might be involved in the pathogenesis of other ciliopathies including polydactyly, craniofacial abnormalities, brain malformation, situs inversus, obesity, diabetes, and polycystic kidney (1, 2).

How does the aberrant ciliary elongation in *Mak*-KO photoreceptors induce progressive photoreceptor death? One possible explanation is that the abnormally elongated cilia affect protein transport from the inner segments to the outer segments in photoreceptors, resulting in photoreceptor degeneration. Several lines of evidence support this idea. We observed an accumulation of rhodopsin in the *Mak*-KO photoreceptor cell bodies in the retina at P14. The transport efficiency of rhodopsin from the inner to the outer segments through the connecting cilia would be reduced in *Mak*-KO photoreceptors. Mutations in rhodopsin or protein transport machinery of the cilia (e.g., *Kif3a* or *IFT* mutants) cause accumulation of rhodopsin in the photoreceptor cell body and result in photoreceptor cell death. Absence of *Dyf-5*, a nematode homolog of *Mak*, affects the motility of kinesin motors and IFT particles in the cilia (14). Similarly, we identified aberrant accumulations of IFT and kinesin in the Mak-KO photoreceptor cilia. Mak may regulate ciliary transport by directly phosphorylating the components of ciliary transport machinery including kinesin and dynein motors, IFT particles, and/or BBSomes (1, 3, 33).

We demonstrate that overexpression of wild-type *RP1* induces ciliary elongation. In addition, expression of the N-terminal portion of RP1 induces an increased intensity of acetylated α-tubulin labeling in cultured cells. These results suggest that excess activation of the microtubule-associated protein RP1 can induce excess ciliary elongation. The evidence shown here supports the idea

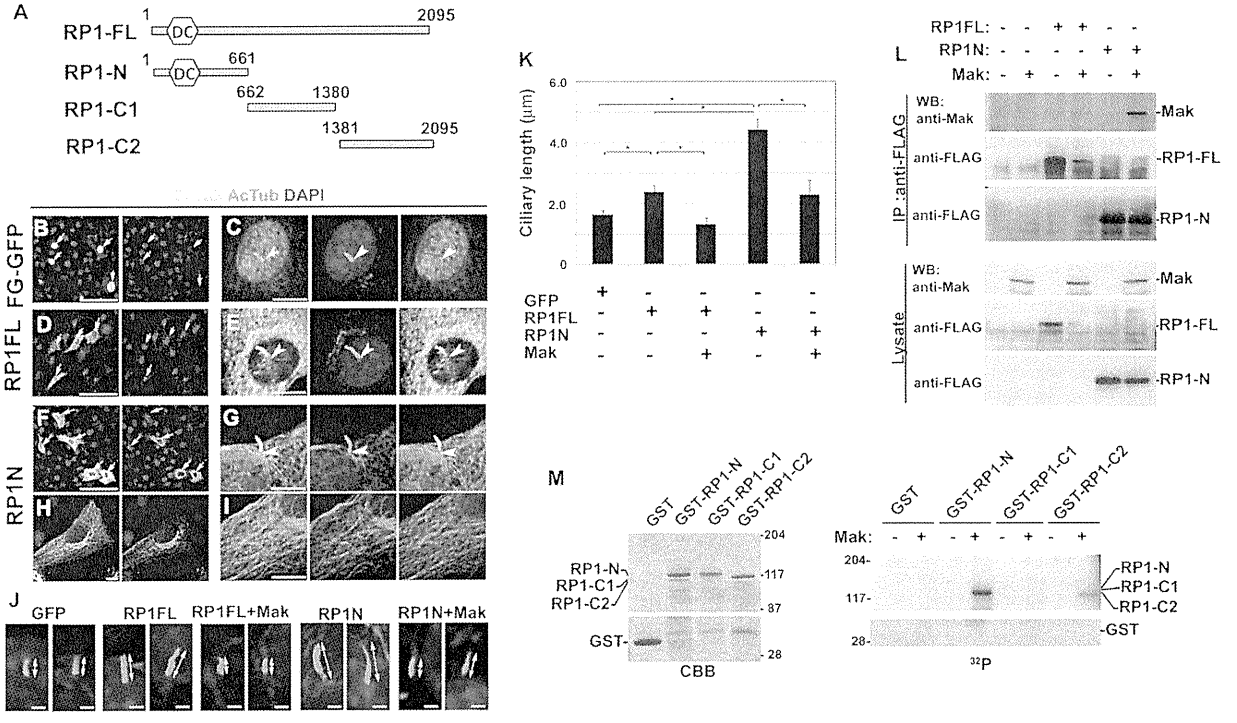

Fig. 4. RP1 controls ciliary length and is phosphorylated by Mak. (*A–I*) Overexpression of RP1 induces ciliary elongation. (*A*) Schematic diagrams of the RP1-FL, -N, -C1 and -C2 constructs. DC, doublecortin domain. (*B–I*) FLAG-tagged constructs expressing GFP (*B* and *C*), RP1-FL (*D* and *E*) or RP1 lacking the C-terminal portion (RP1-N) (*F–I*) were transfected into NIH 3T3 cells. Localization of FLAG-tagged proteins was observed using anti-FLAG (green) and anti-acetylated α-tubulin (red) antibodies and DAPI (blue). Arrows indicate transfected cells. Arrowheads indicate basal part of cilia. (*J* and *K*) RP1 and Mak antagonistically regulate ciliary length. FLAG-tagged constructs expressing GFP, RP1-FL, or RP1-N were transfected with or without a *Mak* expression plasmid into NIH 3T3 cells. (*J*) Cilia were observed using the anti-acetylated α-tubulin (red) antibody. (*K*) The length of the cilia stained with the anti-acetylated α-tubulin antibody ($n > 30$ for each construct). Error bars show SE. $^*P < 0.03$. (*L*) Mak interacts with RP1. A Mak expression plasmid was transfected with or without FLAG-tagged RP1 expression plasmids (RP1-FL or RP1-N) into HEK293 cells. RP1 proteins were immunoprecipitated with the anti-FLAG antibody. Immunoprecipitated Mak was detected by Western blotting analysis using the anti-Mak antibody. (*M*) Mak phosphorylates RP1 in vitro. GST-RP1-N (residues 1–661), GST-RP1-C1 (residues 662–1,380), and GST-RP1-C2 (residues 1,381–2,095) were purified from bacterial extracts and stained with Coomassie brilliant blue (CBB) (*Left*). GST-RP1 deletion proteins were applied for the in vitro kinase assay using purified GST-Mak (*Right*). [Scale bars: 100 μm (*B, D,* and *F*), 10 μm (*C, E, G, H,* and *I*), and 2 μm (*J*).]

that Mak regulates ciliary elongation through RP1 phosphorylation. First, we observed that coexpression of Mak with the RP1 constructs rescued the excess ciliary elongation. Second, we identified that Mak phosphorylates the N-terminal portion of RP1, which contains the doublecortin domain. This domain was originally identified in Doublecortin, whose mutations cause X-linked lissencephaly and double cortex syndrome in humans (34). Interestingly, phosphorylation of Doublecortin by several kinases, including JNK, protein kinase A, and cyclin-dependent kinase 5, was shown to regulate affinity to microtubules and migration of neurons (35, 36). Similarly, it is possible that phosphorylation of RP1 by Mak regulates microtubule stability and controls ciliary length (Fig. S9). Retinitis pigmentosa 1-like 1 (RP1L1), a putative microtubule-associated protein, is another candidate for phosphorylation by Mak (37). In contrast to the restricted localization of RP1 in the axonemes of the outer segments, RP1L1 is localized both in the connecting cilium and the outer-segment axoneme, suggesting its involvement in the mechanisms regulating the length of connecting cilium in photoreceptors. How does Mak affect the intensity of acetylated α-tubulin labeling in the cilia? The first possibility is that the change of microtubule-binding status of microtubule-associated proteins by phosphorylation leads to the activation of enzymes involved in microtubule acetylation or deacetylation, because several microtubule-associated proteins were reported to induce microtubule acetylation (38). The second possibility is that Mak directly regulates enzymes involved in microtubule acetylation and/or deacetylation. It was reported that Aurora A regulates ciliary disassembly before cell-cycle entry through phosphorylation of tubulin deacetylase, histone deacetylase 6 (HDAC6). Phosphorylated by Aurora A, HDAC6 deacetylates microtubules of the cilia and facilitates disassembly of the cilia (39). Furthermore, microtubule acetylation causes the recruitment of the molecular motors dynein and kinesin to microtubules (40). In the developing photoreceptor cilia, regulatory balance of acetylation and deacetylation of ciliary microtubules seems to be important for keeping proper ciliary length and/or ciliary transport machinery. Mak may regulate this balance by phosphorylation of these molecules.

Materials and Methods

Animals. We used *Mak*-KO mice with a deletion of exons 5–8 in the Mak genomic locus which encodes the catalytic kinase domain and the proline and glutamine-rich domain as previously reported (17). The Mak-KO mouse strain was provided by RIKEN BioResource Center through the National BioResource Project of the Japanese Government Ministry of Education, Culture, Sports, Science and Technology. Reagents and procedures are described in detail in *SI Materials and Methods*.

ACKNOWLEDGMENTS. We thank Drs. Y. Shinkai (Kyoto University), T. Li (National Institutes of Health), E. A. Pierce (University of Pennsylvania School of Medicine), J. Zuo (St. Jude Children's Research Hospital, Utah), T. Yamashita (St. Jude Children's Research Hospital), G. J. Pazour (University of Massachusetts Medical School), J. C. Besharse (Medical College of Wisconsin), and H. J. Kung (University of California, Davis) for reagents and technical advice. We thank M. Kadowaki, M. Joukan, A. Tani, T. Tsujii, A. Ishimaru, Y. Saioka, K. Sone, and S. Kennedy for technical assistance. This work was supported by Core Research for Evolutional Science and Technology and Precursory Research for Embryonic Science and Technology from the Japan Science and Technology Agency, a grant from Molecular Brain Science, Grants-in-Aid for Scientific Research on Priority Areas and a Grant-in-Aid for Scientific Research (B), Young Scientists (B), the Takeda Science Foundation, the Uehara Memorial Foundation, Novartis Foundation, Senri Life Science Foundation, Kato Memorial Bioscience Foundation, the Naito Foundation, Mochida Memorial Foundation for Medical and Pharmaceutical Research, and the Japan National Society for the Prevention of Blindness.

1. Gerdes JM, Davis EE, Katsanis N (2009) The vertebrate primary cilium in development, homeostasis, and disease. *Cell* 137:32–45.
2. Nigg EA, Raff JW (2009) Centrioles, centrosomes, and cilia in health and disease. *Cell* 139:663–678.
3. Fliegauf M, Benzing T, Omran H (2007) When cilia go bad: Cilia defects and ciliopathies. *Nat Rev Mol Cell Biol* 8:880–893.
4. Tokuyasu K, Yamada E (1959) The fine structure of the retina studied with the electron microscope. IV. Morphogenesis of outer segments of retinal rods. *J Biophys Biochem Cytol* 6:225–230.
5. Rosenbaum JL, Witman GB (2002) Intraflagellar transport. *Nat Rev Mol Cell Biol* 3: 813–825.
6. Röhlich P (1975) The sensory cilium of retinal rods is analogous to the transitional zone of motile cilia. *Cell Tissue Res* 161:421–430.
7. Hong DH, et al. (2003) RPGR isoforms in photoreceptor connecting cilia and the transitional zone of motile cilia. *Invest Ophthalmol Vis Sci* 44:2413–2421.
8. Marszalek JR, et al. (2000) Genetic evidence for selective transport of opsin and arrestin by kinesin-II in mammalian photoreceptors. *Cell* 102:175–187.
9. Pazour GJ, et al. (2002) The intraflagellar transport protein, IFT88, is essential for vertebrate photoreceptor assembly and maintenance. *J Cell Biol* 157:103–113.
10. Omori Y, et al. (2008) Elipsa is an early determinant of ciliogenesis that links the IFT particle to membrane-associated small GTPase Rab8. *Nat Cell Biol* 10:437–444.
11. Liu Q, Zuo J, Pierce EA (2004) The retinitis pigmentosa 1 protein is a photoreceptor microtubule-associated protein. *J Neurosci* 24:6427–6436.
12. Pierce EA, et al. (1999) Mutations in a gene encoding a new oxygen-regulated photoreceptor protein cause dominant retinitis pigmentosa. *Nat Genet* 22:248–254.
13. Berman SA, Wilson NF, Haas NA, Lefebvre PA (2003) A novel MAP kinase regulates flagellar length in Chlamydomonas. *Curr Biol* 13:1145–1149.
14. Burghoorn J, et al. (2007) Mutation of the MAP kinase DYF-5 affects docking and undocking of kinesin-2 motors and reduces their speed in the cilia of Caenorhabditis elegans. *Proc Natl Acad Sci USA* 104:7157–7162.
15. Bengs F, Scholz A, Kuhn D, Wiese M (2005) LmxMPK9, a mitogen-activated protein kinase homologue affects flagellar length in Leishmania mexicana. *Mol Microbiol* 55:1606–1615.
16. Matsushime H, Jinno A, Takagi N, Shibuya M (1990) A novel mammalian protein kinase gene (mak) is highly expressed in testicular germ cells at and after meiosis. *Mol Cell Biol* 10:2261–2268.
17. Shinkai Y, et al. (2002) A testicular germ cell-associated serine-threonine kinase, MAK, is dispensable for sperm formation. *Mol Cell Biol* 22:3276–3280.
18. Blackshaw S, et al. (2004) Genomic analysis of mouse retinal development. *PLoS Biol* 2: E247.
19. Bladt F, Birchmeier C (1993) Characterization and expression analysis of the murine rck gene: A protein kinase with a potential function in sensory cells. *Differentiation* 53:115–122.
20. Sato S, et al. (2008) Pikachurin, a dystroglycan ligand, is essential for photoreceptor ribbon synapse formation. *Nat Neurosci* 11:923–931.
21. Nishida A, et al. (2003) Otx2 homeobox gene controls retinal photoreceptor cell fate and pineal gland development. *Nat Neurosci* 6:1255–1263.
22. Bascom RA, et al. (1992) Cloning of the cDNA for a novel photoreceptor membrane protein (rom-1) identifies a disk rim protein family implicated in human retinopathies. *Neuron* 8:1171–1184.
23. Hong DH, et al. (2000) A retinitis pigmentosa GTPase regulator (RPGR)-deficient mouse model for X-linked retinitis pigmentosa (RP3). *Proc Natl Acad Sci USA* 97:3649–3654.
24. Liu Q, Lyubarsky A, Skalet JH, Pugh EN, Jr, Pierce EA (2003) RP1 is required for the correct stacking of outer segment discs. *Invest Ophthalmol Vis Sci* 44:4171–4183.
25. Zhao Y, et al. (2003) The retinitis pigmentosa GTPase regulator (RPGR)- interacting protein: Subserving RPGR function and participating in disk morphogenesis. *Proc Natl Acad Sci USA* 100:3965–3970.
26. Mykytyn K, et al. (2004) Bardet-Biedl syndrome type 4 (BBS4)-null mice implicate Bbs4 in flagella formation but not global cilia assembly. *Proc Natl Acad Sci USA* 101:8664–8669.
27. Ross AJ, et al. (2005) Disruption of Bardet-Biedl syndrome ciliary proteins perturbs planar cell polarity in vertebrates. *Nat Genet* 37:1135–1140.
28. Sedmak T, Wolfrum U (2010) Intraflagellar transport molecules in ciliary and nonciliary cells of the retina. *J Cell Biol* 189:171–186.
29. Insinna C, Besharse JC (2008) Intraflagellar transport and the sensory outer segment of vertebrate photoreceptors. *Dev Dyn* 237:1982–1992.
30. Insinna C, Pathak N, Perkins B, Drummond I, Besharse JC (2008) The homodimeric kinesin, Kif17, is essential for vertebrate photoreceptor sensory outer segment development. *Dev Biol* 316:160–170.
31. LaVail MM (1973) Kinetics of rod outer segment renewal in the developing mouse retina. *J Cell Biol* 58:650–661.
32. Xia L, et al. (2002) Identification of human male germ cell-associated kinase, a kinase transcriptionally activated by androgen in prostate cancer cells. *J Biol Chem* 277:35422–35433.
33. Nachury MV, et al. (2007) A core complex of BBS proteins cooperates with the GTPase Rab8 to promote ciliary membrane biogenesis. *Cell* 129:1201–1213.
34. des Portes V, et al. (1998) A novel CNS gene required for neuronal migration and involved in X-linked subcortical laminar heterotopia and lissencephaly syndrome. *Cell* 92:51–61.
35. Schaar BT, Kinoshita K, McConnell SK (2004) Doublecortin microtubule affinity is regulated by a balance of kinase and phosphatase activity at the leading edge of migrating neurons. *Neuron* 41:203–213.
36. Tanaka T, et al. (2004) Cdk5 phosphorylation of doublecortin ser297 regulates its effect on neuronal migration. *Neuron* 41:215–227.
37. Yamashita T, et al. (2009) Essential and synergistic roles of RP1 and RP1L1 in rod photoreceptor axoneme and retinitis pigmentosa. *J Neurosci* 29:9748–9760.
38. Takemura R, et al. (1992) Increased microtubule stability and alpha tubulin acetylation in cells transfected with microtubule-associated proteins MAP1B, MAP2 or tau. *J Cell Sci* 103:953–964.
39. Pugacheva EN, Jablonski SA, Hartman TR, Henske EP, Golemis EA (2007) HEF1-dependent Aurora A activation induces disassembly of the primary cilium. *Cell* 129:1351–1363.
40. Dompierre JP, et al. (2007) Histone deacetylase 6 inhibition compensates for the transport deficit in Huntington's disease by increasing tubulin acetylation. *J Neurosci* 27:3571–3583.

Jpn J Ophthalmol 2010;54:622–637

LETTERS

A Case of Fukuyama Congenital Muscular Dystrophy Associated with Negative Electroretinograms

Fukuyama congenital muscular dystrophy (FCMD) is a congenital dystrophy associated with brain and eye abnormalities.[1] FCMD is an autosomal recessive disorder and occurs only in Japanese. Common ocular findings are optic atrophy, high myopia, cataracts, and weakness of the orbicularis muscles.[1] Abnormal vascular anastomosis and avascularization in the peripheral retina have also been reported. The eyes are only occasionally affected severely, for example, with retinal detachment and microphthalmia.

It was originally believed that patients with FCMD had normal electroretinograms (ERGs),[2] although a slight reduction of the b-wave and reduced ERGs under photopic conditions have been reported.[3,4] We describe an infant with FCMD exhibiting a severe form of ocular phenotype and negative-type ERG under dark-adapted conditions, a finding that to our knowledge has not been reported before.

Case Report

A 1-year-old boy had appeared normal at birth except for a right eye that was slightly microphthalmic. When he was 1 month old, a diagnosis of retinal detachment was made for the right eye (Fig. 1). His left eye was myopic with a tigroid appearance over the entire retina with pallor of the optic disc. The retinal vessels were tortuous, and the temporal peripheral retina was avascularized in both eyes. A scleral encircling buckle and subsequent vitrectomies were used to repair the retinal detachment in the right eye, but the retina remained detached. Before the surgery, the level of creatinine kinase was elevated (3634 IU/l), and the pediatrician suspected congenital muscular dystrophy despite the lack of any distinctive signs or a family history of muscular dystrophy.

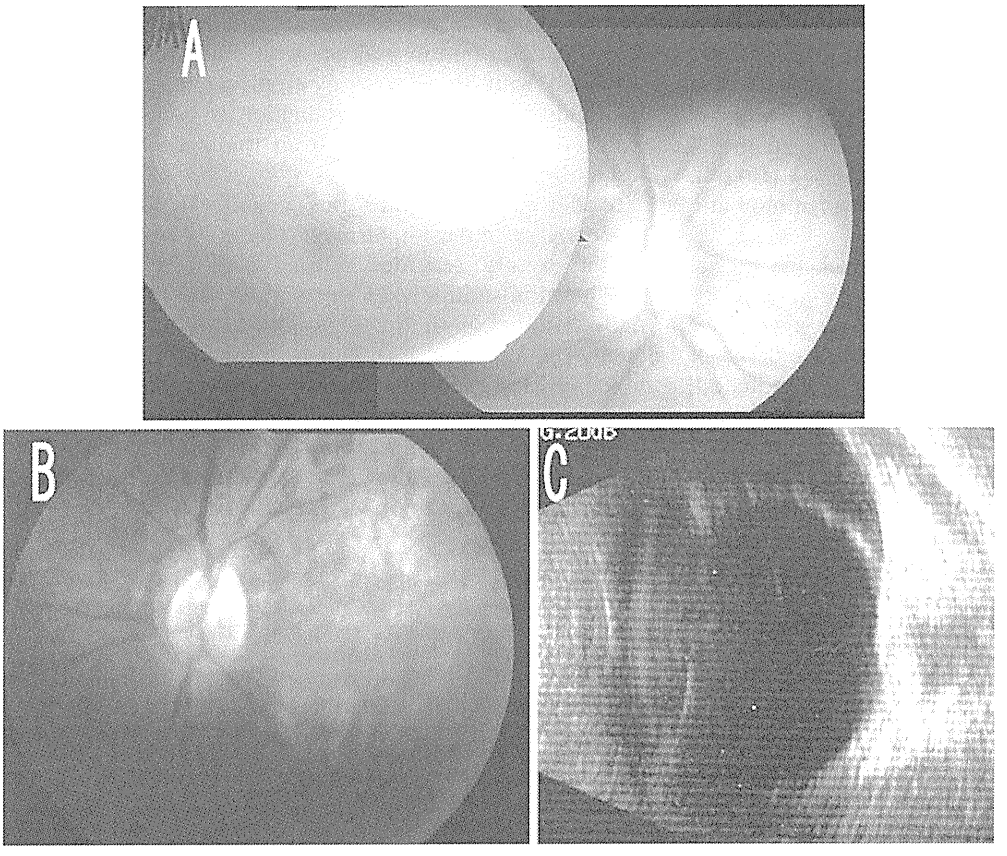

Figure 1A–C. Fundus photographs of our patient with Fukuyama congenital muscular dystrophy (FCMD). **A** Fundus photograph of the right eye showing a temporal retinal detachment involving the macula. **B** Fundus photograph of the left eye showing myopic tigroid appearance with pallor of the optic disc. **C** Ultrasonography showing the retinal detachment in the right eye.

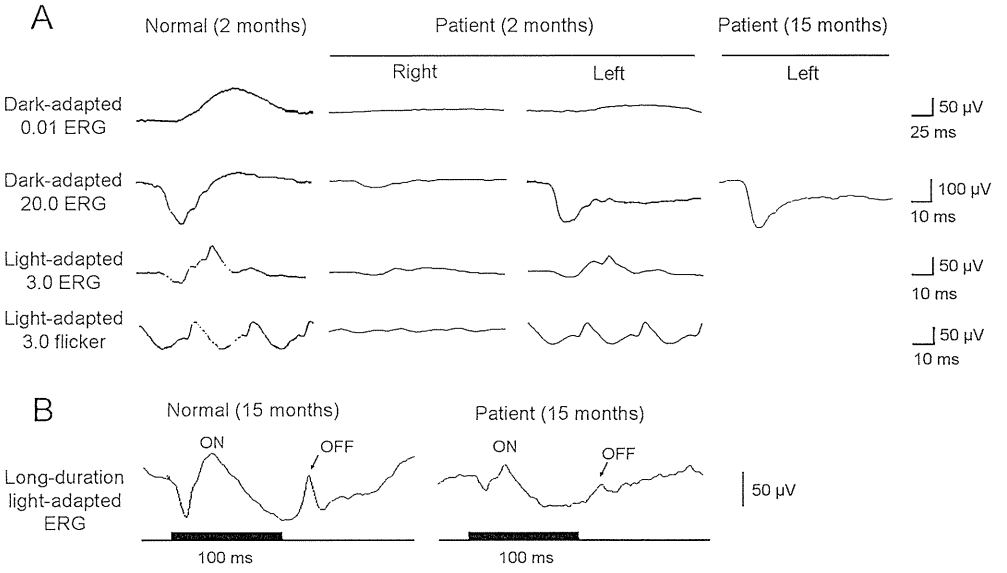

Figure 2A, B. Results of full-field electroretinograms (*ERGs*) using the International Society for Clinical Electrophysiology of Vision-recommended protocol recorded from our patient with FCMD. **A** ERGs recorded in a normal subject at age 2 months (left column), in our patient at 2 months (middle column), and in our patient at age 15 months. The amplitudes of the single-flash cone ERG and 30-Hz flicker ERGs were reduced but better preserved than the rod responses. Note that the maximum rod–cone response (dark-adapted, 20.0 ERG) of our patient showed a "negative" ERG waveform. **B** Light-adapted ERGs elicited by long-duration stimuli in a normal subject at age 15 months (*left*) and in our patient at age 15 months (*right*). Both the ON- and OFF-responses are equally reduced in our patient.

At 5 months, the patient was noted to have muscular weakness and was diagnosed with FCMD. The parents requested genetic testing to confirm the diagnosis. The patient was found to have compound heterozygous mutations in the *FKTN* gene; an insertion mutation in the 3′ noncoding region, and a point mutation, 250C- > T (R47X), in exon 3. The parents were found to be asymptomatic carriers.

During the first vitrectomy under general anesthesia, full-field ERGs were recorded using International Society for Clinical Electrophysiology of Vision-recommended standards (Fig. 2). Because of the retinal detachment, all ERG components in his right eye were severely attenuated. In his left eye, the rod response was decreased to about one-fifth of normal. The a-wave amplitude of the mixed rod–cone ERG was within normal limits, but the b-wave amplitude was smaller than the a-wave amplitude, indicating a negative-type ERG.

Comments

A negative ERG recorded under dark-adapted conditions has not been reported in patients with FCMD and therefore may be a new indication of FCMD. A compound heterozygous mutation in the *FKTN* gene, which occurs infrequently, is most likely the cause of the clinically severe phenotype. This negative-type ERG may be attributable to this less frequent genotype. A similar selective reduction of the b wave was described in patients with muscular dystrophies associated with changes in dystroglycan and dystrophin. The origin of the selective reduction is believed to be a disturbed neurotransmission from the photoreceptors to the ON-bipolar cells.[2]

To determine whether this negative-type ERG was caused by selective impairment of the postsynaptic ON-pathway, we also recorded light-adapted ERGs elicited by long-duration stimuli when our patient was 15 months old. We found that both the ON- and OFF-responses were equally reduced (Fig. 2B). This result is not in accord with the idea that the ON-bipolar cells are selectively disturbed, but an alternative possibility remains that the Müller cells or other neural elements are responsible for the reduction of the b wave because they are also believed to be involved in the generation of the b wave of ERGs.[5]

Acknowledgments. The authors thank Professor Akihiko Tawara for his critical comments and the patient and his parents for their cooperation. This work was partially supported by a Health and Labour Sciences Research Grant (20B-1) for Nervous and Mental Disorders and by Health and Labour Sciences Research Grants for Research on Intractable Diseases from the Ministry of Health, Labour and Welfare of Japan, and by Grants-in-Aid 19592047 and 22591956 for Scientific Research (C) from the Japan Society for the Promotion of Science.

Keywords: *FKTN*, Fukuyama congenital muscular dystrophy, microphthalmia, negative ERG, retinal detachment

Jpn J Ophthalmol
Vol 54: 622–637, 2010

Hiroyuki Kondo[1,2], Kayoko Saito[3], Mari Urano[3], Yukiko Sagara[3], Eiichi Uchio[2], and Mineo Kondo[4]
[1]Department of Ophthalmology, University of Occupational and Environmental Health, Japan, Kitakyushu, Japan; [2]Department of Ophthalmology, Fukuoka University School of Medicine, Fukuoka, Japan; [3]Institute of Medical Genetics, Tokyo Women's Medical University, Tokyo, Japan; [4]Department of Ophthalmology, Nagoya University Graduate School of Medicine, Nagoya, Japan

Received: February 24, 2010 / Accepted: June 29, 2010
Correspondence to: Hiroyuki Kondo, Department of Ophthalmology, University of Occupational and Environmental Health, Japan, 1-1 Iseigaoka, Yahatanishi-ku, Kitakyushu 807-8555, Japan
e-mail: kondohi@med.uoeh-u.ac.jp

DOI 10.1007/s10384-010-0875-0

References

1. Fukuyama Y, Osawa M, Suzuki H. Congenital progressive muscular dystrophy of the Fukuyama type—clinical, genetic and pathological considerations. Brain Dev 1981;3:1–29.
2. Santavuori P, Somer H, Sainio K, et al. Muscle-eye-brain disease (MEB). Brain Dev 1989;11:147–153.
3. Chijiiwa T, Nishimura M, Inomata H, Yamana T, Narazaki O, Kurokawa T. Ocular manifestations of congenital muscular dystrophy (Fukuyama type). Ann Ophthalmol 1983;15:921–923, 926–928.
4. Mishima H, Hirata H, Ono H, Choshi K, Nishi Y, Fukuda K. A Fukuyama type of congenital muscular dystrophy associated with atypical gyrate atrophy of the choroid and retina. A case report. Acta Ophthalmol (Copenh) 1985;63:155–159.
5. Ueda H, Gohdo T, Ohno S. Beta-dystroglycan localization in the photoreceptor and Muller cells in the rat retina revealed by immunoelectron microscopy. J Histochem Cytochem 1998;46:185–191.

Case of a Japanese Patient with X-linked Ocular Albinism Associated with the *GPR143* Gene Mutation

Albinism is an inherited disorder characterized by a reduction or absence of melanin in the hair, skin, and eyes. Albinism can be divided into two broad categories: oculocutaneous albinism and ocular albinism.[1] X-linked ocular albinism (XLOA) is characterized by nystagmus, decreased visual acuity, strabismus, fundus hypopigmentation, macular hypoplasia, and iris hypopigmentation with translucency. It is caused by mutations in the G protein-coupled receptor 143 (*GPR143*) gene (OMIM 300808), originally referred to as the *OA1* gene, which is located at Xp22.32.[2] The fundus of female carriers has a mosaic pattern of pigmentation and depigmentation, which helps in diagnosing XLOA.

We report on a Japanese boy with XLOA whose hair and skin appeared to be hypopigmented, causing some of the referring doctors and his parents to be concerned that he was suffering from oculocutaneous albinism. We detected a *GPR143/OA1* gene mutation, making this the first report of this mutation in Japan.

Case Report

The patient was a 4-month-old boy who had been born by normal delivery with a birth weight of 3148 g. His parents noticed that both his irides were blue and his eye movements appeared abnormal from birth. They consulted a pediatrician, who suspected oculocutaneous albinism. The patient was referred to us when he was 4 months old.

No family history of albinism was reported. His hair was mostly light brown, and his skin color was fair for a Japanese individual. He showed pendular horizontal nystagmus but could follow a slowly moving target. His refraction was –0.50 D = cyl –2.00 D Ax 180° (OD) and –0.50 D = cyl –1.50 D Ax 180° (OS). Slit-lamp examination showed that both irides were light brown (Fig. 1A, B). Bilateral foveal hypoplasia was present, and the ocular fundus was albinotic (Fig. 1C, D). Because his mother's fundus showed a mosaic pattern in the midperiphery, XLOA was diagnosed (Fig. 1E, F). He was also seen by a pediatrician of the Hamamatsu University School of Medicine, who diagnosed oculocutaneous albinism rather than ocular albinism (Fig. 1G, H). Because of the discrepancy in diagnoses, his parents wanted the diagnosis confirmed so as to know whether his skin needed to be protected from ultraviolet exposure.

After genetic counseling, the parents agreed to a genetic examination of their child and of themselves. The molecular genetics study was approved by the Institutional Review Board for Human Genetics and Genomic Research of Hamamatsu University School of Medicine. Nine exons and the surrounding regions of the *GPR143* gene were amplified by polymerase chain reaction (PCR) and directly sequenced. A splice mutation at the junction between exon 5 and intron 5, c.658+1G>A, was detected in the patient (Fig. 2). A heterozygous mutation was detected in his mother, but not in his father. The polymorphisms c.251–135C>T and c.767+10C>G were also detected in the patient.

Comments

This is the first report of a Japanese XLOA patient with a *GPR143* mutation. Various types of mutations in *GPR143* have been identified in Caucasian and Chinese populations. The splice mutation c.658+1G>A that we described here has been previously reported.[3]

Most Japanese patients with XLOA have brown irides that show no translucency, nonalbinotic fundi with moderate pigmentation, and normal skin and hair color.[4] However, the iris in our patient was light brown and the fundus was albinotic. His hair color was mostly light brown, and his skin color was fair for a Japanese individual. The skin and hair pigmentation in Caucasians with ocular albinism can be in the normal range but is frequently lighter in color than that of their siblings without XLOA. Recently, a Chinese family with XLOA and a *GPR143* mutation was reported to have iris hyperpigmentation.[5] Although the amount of pigment

若年者の外傷性白内障手術のポイント

杏林アイセンター
永本　敏之

1．はじめに

眼球外傷は，開放型（open-globe injury）と閉鎖型（closed-globe injury）に分けられ，開放型は更に破裂（rupture，鈍的外傷により眼球壁の弱い部分が破裂した場合），裂傷（laceration，鋭的外傷による眼球壁が全層切れている場合），混合型（破裂と裂傷が混在）に分けられる。更に裂傷は穿孔（penetrating，1箇所が全層切れている場合），眼内異物（intraocular foreign body），二重穿孔（perforating，刺入創と刺出創があり，2箇所で切れている場合）の三つに分けられる。また，閉鎖型は打撲（contusion），表層裂傷（lamellar laceration，全層ではない切り傷や挫滅），表層異物の三つに分けられる[1]（表1）。

表1　眼外傷の分類

開放型（open-globe injury）	閉鎖型（closed-globe injury）
1．破裂（Rupture）	1．打撲（Contusion）
2．裂傷（Laceration）	2．表層裂傷
穿孔（Penetrating）	（Lamellar laceration）
眼内異物	3．表層異物
（Intraocular foreign body）	
二重穿孔（Perforating）	
3．混合型	

次に重症度であるが，開放型のうち角膜のみの裂傷は最も軽く，強角膜裂傷で輪部から5mm後方までの場合が次に軽く，輪部から5mmよりも更に後方に裂傷または破裂が及ぶ場合が最も重症であり，予後不良である[2]。

閉鎖型のうち病変が表層（角結膜，強膜）にしかない場合が最も軽く，前眼部のみに限られるている場合が次に軽く，後眼部にまで及んでいる場合が重症である[1]（表2）。

外傷性白内障は，眼外傷の27～65％に認められる[3-5]。その原因の多くは開放型外傷である（65～88％）[6-8]が，閉鎖型外傷でも起こる。性別は男性に多く，女性の1.9～5.2倍である[9-11]。外傷性白内障とともに後眼部の外傷性病変を伴う確率は48％とい

表2　眼外傷の重症度

開放型（open-globe injury）	閉鎖型（closed-globe injury）
軽症：角膜のみの裂傷	軽症：表層（角結膜，強膜）のみ
中等度：強角膜または強膜裂傷で輪部から5mm後方まで	中等度：前眼部のみ
重症：輪部から5mmよりも更に後方に裂傷または破裂	重症：後眼部にまで及ぶ

う報告[9]もある。眼外傷の視力予後は表2に示した重症度に大きく左右され，網膜，視神経の傷害程度が大きく影響し，次いで角膜，水晶体の光学系の傷害程度が影響する。小児，とくに10歳以下では弱視発症年齢であるため，弱視発症の有無も大きく影響する。眼外傷の病態は症例により様々であり，画一的な治療法があるわけではないが，有用な診察・検査手段を駆使して病状の把握に努め，網膜，視神経の傷害がある場合はその治療が優先される。

開放型眼外傷の治療では，眼球壁の修復が一次的な手術における第一目標となる。開放型軽傷例では角膜のみの損傷であり，角膜縫合をいかに適切に行うかが予後を決める重要な因子である。中等度症例においては輪部から5mm後方までの強角膜または強膜裂傷の適切な縫合が重要である。これらの軽傷・中等度開放型眼外傷例で外傷性白内障を伴っている場合，その治療は縫合と同時に一次手術で行っても二次手術として行ってもよい。ただし，全身麻酔が必要な小児の場合，弱視発生の危険性と麻酔を短期間で二度行うことの全身的な影響も考慮して，一次手術において白内障除去ならびに眼内レンズ（以下IOL）挿入まで行うことが望ましい[5,9,10]。閉鎖型眼外傷では，受傷後ある程度の期間を経て白内障が発症することが多いが，白内障手術時にIOL挿入まで行うべきことは同様である。ただし，開放型や閉鎖型の重症例で後眼部も障害されている場合で，外傷性白内障がある場合は後眼部病変の治療を第一優先とし，状況が許せばIOL挿入まで行うという方針にすべきである。

以下に杏林アイセンター（以下 当センター）での若年者の外傷性白内障手術について報告する。

2. 当センターにおける若年者の外傷性白内障の治療

対象は1999年6月～2009年10月の期間に，外傷性白内障に対して手術を行い術後3カ月以上経過観察ができた19歳以下の11例11眼であった。性別は男児が8例8眼，女児が3例3眼（男/女＝2.67）で，手術時の平均年齢は8.2±6.4歳（0～19歳）であり，術後平均観察期間は53±40カ月（3～134カ月）であった。鈍的（閉鎖型）外傷群と穿孔性（開放型）外傷群に分けて検討したが，鈍的外傷は4眼（36.4％），穿孔性外傷は7眼（63.6％）で，全例片眼性であった。男児に多いこと，穿孔性が多いことはこれまでの報告と同様である。

まず，鈍的外傷群の4例4眼（表3）であるが，年

表3　鈍的（閉鎖型）外傷例の術前所見

症例	手術時年齢（歳）	性別	受傷機転	虹彩離断	前嚢破裂	チン小帯断裂	前房出血	網膜剝離	外傷－手術期間（月）
1	11	男	木の棒	－	－	（＋）	－	－	96
2	11	男	ゴムバンド	－	－	（＋）	－	－	5.5
3	18	男	ソフトボール	（＋）	（＋）	－	（＋）	－	1.2
4	19	男	野球	－	－	（＋）	－	（＋）	10

表4　鈍的（閉鎖型）外傷例の術式と術後の状態

症例	術　式	IOL固定	術後最終視力	術後SE変化（患眼/健眼）	術後乱視（患眼/健眼）	術後観察期間（月）
1	IA＋AV＋IOL縫着	嚢外	1.2	－2.00 /－0.63	0.50/0.50	94
2	PEA＋CTR＋IOL	嚢内	1.2	0.75 /0.25	0.50/0	28
3	虹彩縫合＋IA＋IOL	嚢内	0.8	－1.00 /－0.75	0/1.50	72
4	PEA＋SS－CTR＋IOL	嚢内	1.2	－0.88 /0.13	0.75/0.25	3

IA：吸引術，AV：前部硝子体切除術，IOL：眼内レンズ，PEA：超音波水晶体乳化吸引術，CTR：水晶体嚢拡張リング，SS-CTR：部分縫着型水晶体嚢内リング，SE：等価球面度数

表5　穿孔性（開放型）外傷例の術前所見

症例	年齢（歳）	性別	受傷機転	穿孔創	前嚢穿孔	後嚢穿孔	虹彩穿孔	網膜穿孔	前房出血	外傷－手術期間（日）
5	0.2	男	不明（針？）	角膜	（＋）	（＋）	（＋）	（＋）	－	3
6	2	女	はさみ	角膜	（＋）	（＋）	－	－	（＋）	0
7	3	女	シャーペン	角膜	（＋）	－	－	－	－	0
8	3	男	はさみ	角膜	（＋）	－	－	－	－	0
9	4	男	不明	角膜	（＋）	（＋）	（＋）	－	－	30
10	5	男	不明	強角膜	－	－	－	－	（＋）	1,022
11	14	女	ワイヤー	角膜	（＋）	－	－	－	－	1

表6　穿孔性（開放型）外傷例の術式と術後の状態

症例	術　式	IOL固定	術後最終視力	術後SE変化（患眼 健眼）	術後乱視（患眼 健眼）	術後観察期間（月）
5	PEA＋PPC＋AV＋IOL	嚢内	測定不能	－9.20 －1.50	0.75 0.12	23
6	IA＋AV＋角膜縫合	－	1.2	－3.50 －0.125	0.25 0.25	47
7	IA（2nd IOL）	嚢内	1.2	－5.25 0.75	0.50 0	91
8	PEA＋PPC＋AV＋IOL＋角膜縫合	嚢内	1.2	－8.00 －3.625	2.00 1.25	134
9	PEA＋PPC＋AV＋IOL	嚢内	1.0	－0.625 0.125	0.50 0.50	3
10	SL＋MS＋PEA＋PPC＋AV＋IOL	嚢内	手動弁	測定不能	測定不能	24
11	PEA＋IOL	嚢内	1.0	－1.25 －0.875	4.50 1.25	68

PPC：一次的後嚢切除，2nd IOL：二次的IOL挿入術，SL：虹彩後癒着剝離，MS：瞳孔括約筋放射状多数切開

齢は全例11歳以上で全例男児であった。受傷機転はスポーツに起因するものが多かった（症例2のゴムバンドはトレーニング用）。併発症はチン小帯断裂が最も多く3眼に認められ，その他は前嚢破裂，前房出血，虹彩離断，網膜剝離が各1眼であった。受傷から手術までの期間は，全例1カ月以上経っており，平均28.8カ月と長かった。術式と術後の状態を表4に示した。網膜剝離を併発していた症例4は，強膜バックル手術で網膜が復位した後に白内障手術を施行していた。チン小帯断裂の3例では水晶体嚢拡張リングがない時代には，前部硝子体切除とIOL縫着で対処し，最近は水晶体嚢拡張リング，または部分縫着型水晶体嚢内リング＋IOL嚢内固定で対処していた。虹彩離断に対しては10－0プローリンで縫合整復を行っていた。前嚢破裂が併発した1例は，小さな破裂が周辺部に開いていたため，そこを避けて，その内側にcontinuous curvilinear capsulorrhexis（以下 CCC）を行って対処していた。術中合併症を認めたのは症例1で，前嚢亀裂を生じ後嚢にまで回って後嚢破損となった1眼のみであった。術後合併症は，高眼圧を1例（症例3）に認めるものの，点眼治療にて眼圧は正常で，緑内障性視野変化も認めていない。術後視力は全例0.8以上で，手術時年齢が比較的低かった症例1では長期観察例により健眼よりもわずかに強い近視化を認めるものの，眼鏡で十分対処可能であった。また閉鎖型外傷であるため，術後乱視は軽度であった。

次に穿孔性（開放型）外傷例の7例7眼であるが，鈍的外傷より全体的に低年齢で，6例が6歳未満であり弱視好発年齢であった（表5）。手術時平均年齢は，鈍的外傷で14.8歳，穿孔性外傷で4.5歳であり，有意差（Welchのt検定，$p=0.0084$）を認めた。鈍

的外傷が男児に多かったのに対し，穿孔性では性差を認めなかった。低年齢のため受傷機転不明の場合も多かった（表5）。穿孔創は，症例10以外の6例は角膜穿孔で，症例10は強角膜穿孔であった。併発症として前嚢穿孔は6例，後嚢穿孔3例，虹彩穿孔2例，網膜穿孔1例，前房出血2例を認め，受傷後約3年で手術をした症例10は，虹彩炎，虹彩前・後癒着，角膜混濁を伴っていた（表5）。症例10を除いては，開放型のため受傷後早期（5例は3日以内，1例は30日目）に白内障手術を施行しており（表5），5例は初回手術時にIOLを挿入し，1例は受傷後1カ月で二期的に挿入していた（表6）。穿孔創の処置は，小さな角膜穿孔創であったため縫合しなかったのが4例で，角膜または強角膜を縫合したのが3例であった。前嚢穿孔があっても全例でCCCが完成でき，後嚢穿孔があった3例中2例は後嚢CCCが可能であった。白内障除去の術式として，5例で超音波水晶体乳化吸引術（以下 PEA）を用いており，これら5例はIOLを嚢内に固定していた。このうち14歳の1例を除いた4歳以下の4例で後発白内障の予防策として後嚢CCC＋前部硝子体切除を施行していた。初回手術で前嚢CCCと吸引術（以下 IA）を行った症例7は，1カ月後二期的に後嚢切除と前部硝子体切除を行い，IOLを嚢内に挿入していた。また下方角膜の裂傷で角膜縫合とPEA，前部硝子体切除術を初回手術時に行った症例6は，虹彩損傷と後嚢損傷が大きく，IOLは挿入せず，術後コンタクトレンズ（以下 CL）装用にて経過観察中である（表6）。術中合併症は，今回の症例では認められていない。症例10のみは特殊で，初診時年齢2歳2カ月で左眼8時の輪部付近の強角膜裂傷で虹彩が脱出陥頓しており，初回手術として強角膜縫合術を行い，眼鏡処方と健眼遮蔽により術後4カ月で視力（0.5）まで回復したものの，術後穿孔創に虹彩前癒着があり，創付近の角膜は徐々に混濁が広がり，術後2年1カ月で続発性閉塞隅角緑内障を発症し，薬剤で眼圧をコントロールしようとするも不十分で，創付近のデスメ膜瘤を来し，帯状角膜変性も出現，更に白内障が出現・進行し，視力（0.01）まで低下した症例である。二次手術としてEDTA（エチレンジアミン四酢酸）による帯状角膜混濁除去と創付近の表層角膜移植を施行し，その2週間後に三次手術として緑内障に対する隅角癒着解離術と，瞳孔処置として虹彩後癒着剝離＋瞳孔括約筋多数切開，白内障に対するPEA＋後嚢切除＋前部硝子体切除＋IOL嚢内固定を行い，視力は一時（0.2）まで回復したものの，その後角膜混濁が拡大・進行し，現在術後5年1カ月で視力は手動弁にとどまっている。この1例と現在まだ2歳で視力が測定できない1例を除いた5例は（1.0）以上の視力を得ている（表6）。術後の成長に伴う近視化は，低年齢でIOLを挿入した患眼では健眼よりも強く認められた。穿孔にもかかわらず術後乱視はそれほど強くなかった（表6）。

3．小児外傷性白内障に対する手術のポイントーその1

外傷性白内障の手術は，老人性白内障に対する手術とは大きく異なり，患者の病状に合わせて他の眼合併症への対処が必要であるとともに，白内障に関しても手術方法，粘弾性物質，機械の設定値など適宜選択する必要がある。このため術者の知識と技量が大きく予後を左右し，手術器具と機械，設備の充実度も影響する。とくに小児の場合は，手術が難しい上に弱視の危険性もあるため予後不良となりやすい。これまで報告されている小児の外傷性白内障の治療成績では，術後の視力が（0.5）以上になる割合は45～70％であり，50％前後の報告が多い[6,7,10,11]。しかし今回の杏林アイセンターの成績では，11眼中測定不能の1眼を除くと10眼中9眼で（0.8）以上，8眼で（1.0）以上と非常に良好な成績が得られた。

冒頭でも述べたように全身麻酔が必要な小児の場合，弱視発生の危険性，麻酔を短期間で二度行った場合の全身的な影響なども考慮して，一次手術において白内障除去ならびにIOL挿入まで行うことが望ましいとされている[3,9,10]が，今回の11症例中，特殊例の症例10を除いた10例中8例で一次手術においてIOLが挿入されており，残りの2例中1例は1カ月後に二次的に挿入され，他の1例はCL装用により，術後の矯正が適切にされ，必要に応じて健眼遮蔽がされていたことも良好な成績に貢献したと思われる。

4．小児外傷性白内障に対する手術のポイントーその2（閉鎖型眼外傷）

小児・若年者の鈍的外傷による閉鎖型眼外傷に伴う白内障において伴いやすい併発症は，チン小帯断裂，後嚢破裂，虹彩離断，前房出血である。これらの併発症に対する処置が重要である。

前房出血がある外傷性白内障の場合，弱視発症年齢（10歳未満）においては，外傷後1週間程度で手術を行うが，それ以降の年齢では保存的療法で出血が引くのを待って眼内の状況をよく把握してから手術を行う。また，前房が出血で埋め尽くされコントロール不能の眼圧上昇がある場合や超音波検査で網膜剝離を伴っている場合には，早期に前房出血（と網膜剝離）に対して手術を行う。ただし，再出血を来しやすいとされる外傷後5日間はなるべく手術を避ける。2箇所のサイドポートから挿入したバイマニュアルIAで前房出血を除去し，前房内に粘弾性物質を注入した後に眼内の状況をよく観察し，その後の手術法を決める。

チン小帯断裂を伴っている場合は，断裂範囲の把握と前房内への硝子体脱出の状況がまず重要である。断裂範囲が90°以内で比較的狭い場合は，硝子体脱出を伴わないか，伴っているとしてもわずかである。サイドポートから粘弾性物質を注入して硝子体を押し戻してふたをするが，サイドポート作成時も粘弾性物質注入時も前房を虚脱させないことがまず重要である。前房虚脱は硝子体脱出を助長してしまうからである。すでに硝子体が脱出している場合は，ヒーロンV[3]で脱出硝子体を硝子体腔に押し戻し，更に押し戻した硝子体上とチン小帯断裂範囲を覆うようにビスコート[3]を注入してから，眼圧が正常範囲になるようにヒーロンVで前房内全置換を行い，房水を完全排除する。次に2.4mm強角膜自己閉鎖創を作成し，サイドポートからチストトームまたは前嚢鑷子を刺入して直径5.0mmのCCCを作成する。断裂範囲が広い場合には，サイドポートから刺入したプッシュアンドプルフックをCCC縁に引っ掛けてカウンターとなる力を加えつつ，鑷子でCCCを作成する。次に高分子量粘弾性物質で360°ビスコダイセクションを行い，前嚢と最表層皮質を分離する。次に後端のアイレットに長い10－0ナイロンを通糸した水晶体嚢拡張リングを水晶体嚢赤道部に挿入する。このときにビスコダイセクションで分離した空隙にリングを挿入し，リングと前嚢の間に皮質を挟まないことと，挿入中のリングの位置がなるべく赤道部付近となるようにサイドポートから挿入したフックでコントロールすることにより，チン小帯への負荷をかけないことが重要である。下手な挿入をするとチン小帯断裂を助長してしまったり，皮質がリングと前嚢の間に挟まって除去が難しくなったりしてしまう。後端アイレットに通した10－0ナイロンは，リングを除去しなければならなくなったときのためのライフラインである。長いまま邪魔にならないような位置に置き，術中に引っ掛けないように気をつける。その後最小限のハイドロダイセクションにより皮質を後嚢から分離する。ヒーロンV下の過量注入は極端な眼圧上昇をもたらすため禁忌である。次にフェイコで水晶体内容を除去するが，前房内のヒーロンVを残すために吸引流量20cc/min未満，最大吸引圧200mmHg未満，ボトル高50cm以下に設定する。うまくビスコダイセクションができていれば，フェイコだけで皮質はほとんど残らない。わずかに残った皮質をIAで除去する。その後IOLを嚢内に挿入するが，6歳以下の場合はその前に後発白内障予防のために後嚢CCCと25ゲージ（以下G）前部硝子体切除（カット数800cuts/min，吸引圧400 ～ 500mmHg，ボトル高60cmが筆者の設定である）を行う。IOLを問題なく挿入できたら，ライフラインとして残しておいた10－0ナイロンを切除する。その後ボトル高50cm以下で粘弾性物質を除去し，IAチップを抜いた直後に切開創を人差し指で押さえて前房虚脱を防ぎ，サイドポートからbalanced salt solution（以下 BSS）を注入して眼圧をいったん高めにしてから少し漏出させて正常化し，サイドポートと切開創の自己閉鎖を確認し，もし閉鎖していなければハイドレーションで閉鎖させ，眼圧を正常化して結膜を切開創にかぶせて縫合する。リン酸デキサメタゾンナトリウム（デカドロン）を結膜下に注射し，オフロキサシン（タリビッド）眼軟膏を点入し，眼帯をして手術終了である。

断裂範囲が90°以上である場合は，縫着による支

えが必要であるため，まず縫着用の強膜フラップを断裂範囲の中央に作成する．1～5時の断裂であれば3時ということになるが，3時と9時は縫着で硝子体出血を来す危険性が高いため，この場合は2時にずらす．断裂範囲が180°以上である場合は，この強膜フラップの180°対側にもう一つ強膜フラップを作成する．断裂範囲が90°以上である場合は，かなりの量の硝子体が前房内に脱出していて硝子体腔への押し戻しが不可能であることが多いため，両サイドポートからの25G硝子体カッターによる脱出硝子体のバイマニュアルビトレクトミーを行う．硝子体切除後に上記と同様にビスコートとヒーロンVで前房を置換し，それでも眼圧が低い場合は，チン小帯断裂領域からBSSを硝子体内に注入して眼圧を正常化させる．前房内はヒーロンV，断裂範囲上はビスコート，硝子体内はBSSという状況を作る．前述のごとく強角膜切開創作成後CCCを作成し，ビスコダイセクションを行う．断裂が180°未満の場合は，部分縫着型水晶体嚢内リング（タイプ6D，Morcher社）を縫着後，通常の水晶体嚢拡張リングを挿入し，断裂が180°以上240°未満の場合は縫着リング（タイプ2L，Morcher社）を縫着する．その後は上記と同様にハイドロダイセクション後に水晶体を除去し，IOLを嚢内固定する．ただし断裂が180°以上の場合は，タイプ2Lでの対処以外に水晶体金切除術や経毛様体水晶体切除術，水晶体嚢内摘出術も考慮する．

後嚢破裂がある場合は，白内障が徐々に進行する場合が多いのと破裂縁が外傷後6週間以上で線維化する場合が多く[7]，線維化した方が術中に破嚢の拡大が起きにくく手術がやりやすいため，視力の状態に応じてではあるが，なるべく待って手術をする．手術ではハイドロダイセクションは行わず，水晶体中心部を除去後にビスコダイセクションで水晶体周辺部を嚢から分離し，破裂部上にビスコートを注入後，低吸引低灌流で水晶体周辺部を除去する．必要に応じて後嚢CCCと前部硝子体切除を追加してなるべく嚢内にIOLを挿入する．後嚢の残存が不十分で嚢外に固定する場合は，3ピース球面IOLを用いてCCCサイズに応じて光学部径を選択し，嚢外に挿入してから光学部をCCCにキャプチャー（anterior optic capture）する．

虹彩離断の場合は，瞳孔偏位の程度に応じて修復するかどうか決定する．

5．小児外傷性白内障に対する手術のポイントーその3（開放型眼外傷）

開放型眼外傷による外傷性白内障の治療でまず重要なのは，穿孔創を修復するための適切な（強）角膜縫合である．ただし創が自然閉鎖している場合は，もちろん縫合の必要はない．創が小さくヒーロンVが創から漏出せず前房が保てる場合は，まず白内障手術を行ってから創を縫合する．前房が保てない場合は創を縫合してから白内障手術を行う．創縫合の基本は10－0ナイロンの端々縫合で，通糸方向は創方向に直角（V字，Y字の創は図1），深さは2/3程度に深く，最低でも1/2以上深くなければならない．

前嚢裂傷に対する処置としては，裂傷が小さければCCC内に裂傷を入れてしまえばよい．裂傷が大きく周辺部まで伸びている場合は，八重式剪刀でCCCのきっかけとなる切開を裂傷部に作成後にサイドポート鑷子でCCCを作成し，1 tearまたは2 tear CCCの形とする．安定したIOLの固定を得るためには前嚢CCCの可否が重要であるが，CCCが流れやすい小児・若年者においては粘度が高く漏出しにくいヒーロンVと，サイドポートから挿入できるため粘弾性物質が漏れにくいサイドポート前嚢鑷子を用いることにより，たとえ前嚢穿孔があったとしてもほとん

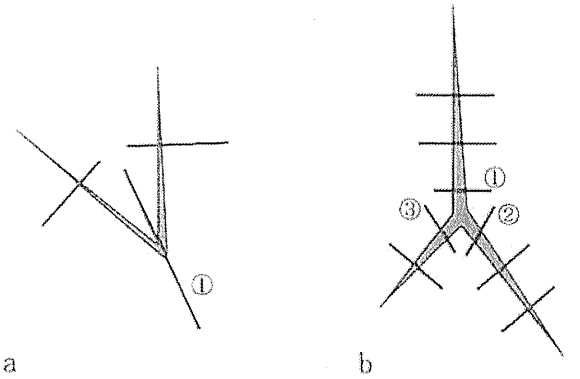

図1　角膜穿孔創の縫合
a：V字の裂傷の場合，頂点方向の縫合（①）後に創方向に直角の方向の縫合を置く．b：Y字の切創では，Yの中心部を短い縫合（①～③）で寄せてから，創方向に直角の方向の縫合を置く．

どすべての症例でCCCが可能である。Tearが後嚢まで伸びて後嚢破損にまで進展することを防ぐためには，術中の前房内圧変動を極力抑えることが重要で，そのためには，ハイドロダイセクションを行わないこと，低灌流・低吸引に設定すること，前房虚脱を防ぐこと（チップを抜く際には人差し指で切開創を押えてしまう）がポイントとなる。

後嚢裂傷がある場合は，鈍的外傷の項で述べた後嚢破裂と同様に対処する。

6. おわりに

以上，小児の外傷性白内障の手術のポイントについて述べた。以上のポイントは日ごろから先天白内障の手術を行ってIOLを挿入している術者にとっては，共通する項目が非常に多く比較的容易であるが，成人の白内障手術しか行っていない術者や先天白内障手術でもIOLを挿入しない手術しか行っていない術者にとっては，いざ行うとなっていきなり行えるものではなく，かなり難しいと思われる。したがって，小児の外傷性白内障でとくに6歳以下の場合は，小児のIOL手術を多く手掛けている施設に紹介する方が賢明であると思われる。

文　献

1) Pieramici DJ, Sternberg P Jr, Aaberg TM Sr, et al : A system for classifying mechanical injuries of the eye (globe). The Ocular Trauma Classification Group. Am J Ophthalmol, **123** : 820-831, 1997.
2) May DR, Kuhn FP, Morris RE, et al : The epidemiology of serious eye injuries from the United States Eye Injury Registry. Graefes Arch Clin Exp Ophthalmol, **238** : 153-157, 2000.
3) Dannenberg AL, Parver LM, Brechner RJ & Khoo L : Penetration eye injuries in the workplace. The National Eye Trauma System Registry. Arch Ophthalmol, **110** : 843-848, 1992.
4) Slusher MM, Greven CM & Yu DD : Posterior chamber intraocular lens implantation combined with lensectomy-vitrectomy and intraretinal foreign-body removal. Arch Ophthalmol, **110** : 127-129, 1992.
5) Rumelt S & Rehany U : The influence of surgery and intraocular lens implantation timing on visual outcome in traumatic cataract. Graefes Arch Clin Exp Ophthalmol, **248** : 1293-1297, 2010.
6) Staffieri SE, Ruddle JB & Mackey DA : Rock, paper and scissors? Traumatic paediatric cataract in Victoria 1992-2006. Clin Experiment Ophthalmol, **38** : 237-241, 2010.
7) Karaman K, Znaor L, Lakos V & Olujic I : Epidemiology of pediatric eye injury in Split-Dalmatia County. Ophthalmic Res, **42** : 199-204, 2009.
8) Kumar S, Panda A, Badhu BP & Das H : Safety of primary intraocular lens insertion in unilateral childhood traumatic cataract. JNMA J Nepal Med Assoc, **47** : 179-185, 2008.
9) Kuhn F : Traumatic cataract : What, when, how. Graefes Arch Clin Exp Ophthalmol, **248** : 1221-1223, 2010.
10) Churchill AJ, Noble BA, Etchells DE & George NJ : Factors affecting visual outcome in children following unilocular traumatic cataract. Eye (Lond), **9** : 285-291, 1995.
11) Brar GS, Ram J, Pandav SS, et al : Postoperative complications and visual results in unilocular pediatric traumatic cataract. Ophthalmic Surg Lasers, **32** : 233-238, 2001.
12) Cheema RA & Lukaris AD : Visual recovery in unilateral traumatic pediatric cataracts treated with posterior chamber intraocular lens and anterior vitrectomy in Pakistan. Int Ophthalmol, **23** : 85-89, 1999.
13) Gupta AK, Grover AK & Gurha N : Traumatic cataract surgery with intraocular lens implantation in children. J Pediatr Ophthalmol Strabismus, **29** : 73-78, 1992.
14) Brady KM, Atkinson CS, Kitty LA & Hiles DA : Cataract surgery and intraocular lens implantation in children. Am J Ophthalmol, **120** : 1-9, 1995.
15) Vajpayee RB, Angra SK, Honavar SG, et al : Pre-existing posterior capsule breaks from perforating ocular injuries. J Cataract Refract Surg, **20** : 291-294, 1994.
16) Thomas R : Posterior capsule rupture after blunt trauma. J Cataract Refract Surg, **24** : 283-284, 1998.

（別刷請求先）永本敏之　〒181-8611　三鷹市新川6-20-2　香林アイセンター

綜説

先天白内障の外科的治療

—Surgery for congenital cataracts—

永本敏之*

はじめに

先天白内障の治療法は最近大きな変革を遂げ，ある程度良好な予後が期待できるようになった．しかし，良好な術後状態を得るためには，手術に関する高度な知識と技量が要求されるため，小児の白内障手術に長けた術者と小児眼科，特に弱視治療の専門家（医師または視能訓練士）との協力体制で治療に当たることが望ましい．

I. 手術適応と時期

現状では手術治療以外に確実な治療手段がないためほとんどの症例が手術適応であるが，術者の技量と術後の管理の問題も鑑みて手術によって現状と同じかより良好な視機能が得られる可能性が高いと考えられる場合に適応となる．たとえば3歳で混濁が軽度で視力が(0.8)という場合には手術による視力向上は期待できず，調節力を失い，術後の眼軸長延長に伴う近視化などを考えるとデメリットのほうが大きく，手術適応とはならない．しかし3歳で混濁が中等度で視力が(0.2)であれば，手術適応と考える．

視力の発達には左右眼における競争原理が強く働いている．つまり，白内障の混濁により網膜像が劣化し，さらに混濁に左右差があると，ヒトは網膜像の良好なほうの眼を使う．その結果，混濁の弱いまたはない眼では，網膜からのニューロンの活動が盛んとなり，他眼の混濁の強い眼からのニューロン活動は微弱であるため，ニューロンの活動が盛んな混濁の弱い眼からの大脳皮質視覚野におけるシナプスが優先的に形成され，視力の良好な発達につながる．一方，混濁の強い眼からのニューロンは，大脳皮質視覚野でのシナプス形成が不良となり，視力の発達も不良となる．つまり，混濁に左右差があるかどうかが弱視の発生の大きなポイントであり，混濁の差に応じて弱視の程度も決まる．ただし，両眼ともに瞳孔領を隠す強い混濁がある場合は，両眼とも弱視となる．このような弱視は混濁によって形態覚が遮断（障害）されることによって発生するため形態覚遮断弱視と呼ばれる．視力の発達には生後間もない時期が非常に重要であり，生後3～4カ月までには網膜のニューロンと大脳皮質の神経細胞とのシナプスが完成してしまう．さらにこの中でも生後1～2カ月が特に重要であり，片眼性の強い混濁の場合，左右眼のシナプス形成に圧倒的な差ができてしまうため，生後6週までに手術しないと視力向上はあまり期待できない．このように先

* Toshiyuki NAGAMOTO　谷林アイセンター

Key words：先天白内障，眼内レンズ，形態覚遮断弱視，congenital cataract, Intraocular lens, form vision deprivation amblyopia

表1　形態覚遮断弱視治療の臨界期

片/両	臨界期
片眼性	生後6週
両眼性	生後10～14週

表2　両眼性白内障の混濁形状と形態覚遮断弱視

混濁形状	形態覚遮断弱視
層状白内障	軽度
前極白内障	
後極白内障	
核白内障	重度
全白内障	

表3　先天白内障治療の3本柱

混濁除去(手術)
屈折矯正(眼内レンズ，眼鏡，コンタクトレンズ)
弱視訓練(健眼遮閉)

天白内障による形態覚遮断弱視では，治療の時期の限界があり，これを臨界期と呼んでいる。片眼性または左右差の強い両眼性の場合には6週であるが，左右差があまりない両眼性の強い混濁の場合は10～14週と考えられている(表1)。

手術時期の決定には，形態覚遮断弱視が発生しているのかどうか，もしあるならばどの程度なのかが問題である。視力が測れない2歳以下あるいは知的障害のある患児の場合，弱視の程度の予想は混濁の形状と部位，濃さ，そして左右差による。たとえば両眼性の層状白内障，前極白内障，後極白内障は軽度弱視の場合が多いが，核白内障がある場合や全白内障は強い弱視になりやすい(表2)。強い弱視が疑われれば，できるだけ早急に手術とする。強い弱視が疑われ，臨界期も過ぎている場合は予後不良(0.1以下)が予想されるが，生直後に既に強い混濁があったかどうかは不明で，もし生直後は混濁がないか弱かった場合は，良好な視力が得られる可能性もあるため，中等度の弱視が疑われる場合も早期に手術とする。弱視がないかあっても軽度と予想される場合は，眼球の成長を待って2歳以降，できれば8歳以降に手術とする。手術時期の決定には豊富な知識と経験，そして待つ場合は勇気が必要である。また，注意深い経過観察が必要であり，白内障が進行すれば早めの手術が必要となる。

II. 基本的治療法

先天白内障に対する基本的治療の3本柱は，混濁の除去(瞳孔領の透明性確保)，適切な屈折矯正(2歳まで眼前1m，それ以降は遠近両用で矯正)，健眼遮閉(弱視訓練)である。そして問題となるのは，手術方法，屈折矯正方法(眼内レンズ，コンタクトレンズ，眼鏡)である(表3)。

III. 手術の基本方針

2011年1月現在において，私が考えている最良の方法は眼内レンズ(IOL)を嚢内挿入して，術後は眼鏡で矯正する方法である。簡潔に術式を述べると，切開は3mm以下の強角膜自己閉鎖創で，4～5mm程度の前嚢CCC(continuous curvilinear capsulorrhexis)(年齢によって大きさが異なる)，超音波乳化吸引装置を用いた吸引術，3～4mm程度の後嚢CCC(または25Gカッターによるposterior capsulectomy)，25Gカッターによる前方1/4～1/3程度の硝子体切除，直径5.5～6.0mmのアクリルIOL嚢内挿入である。ただし8歳以降は術後のYAGレーザーが可能であるため後嚢切開と前部硝子体切除は行わず，成人と同様にシャープエッジのアクリルレンズを嚢内に挿入する。以前は，経毛様体水晶体切除術が推奨されたこともあるが，